LA-UR-21-21184
Approved for public release; distribution is unlimited.

Title: Self-Seeding, Regenerative Amplifier FEL & XFELO

Author(s): Nguyen, Dinh C.
Anisimov, Petr Mikhaylovich
Li, Yuanshen
Neveu, Nicole

Intended for: USPAS 21 lecture slides

Issued: 2021-02-09

VUV and X-ray Free-Electron Lasers

Self-Seeding, Regenerative Amplifier FEL & XFELO

Dinh C. Nguyen,[1] Petr Anisimov,[2] Yuanshen Li,[3] Nicole Neveu[1]

[1] SLAC National Accelerator Laboratory

[2] Los Alamos National Laboratory

[3] University of Chicago

Monday (February 1) Lecture Outline

	Time
• X-ray diffraction in crystals	10:00 – 10:20
• Hard X-ray self-seeding	10:20 – 10:50
• Break	10:50 – 11:00
• Soft X-ray self-seeding	11:00 – 11:20
• Regenerative Amplifier FEL	11:20 – 11:40
• XFELO	11:40 – Noon

X-ray Diffraction in Crystals

Diffraction from an Aperture

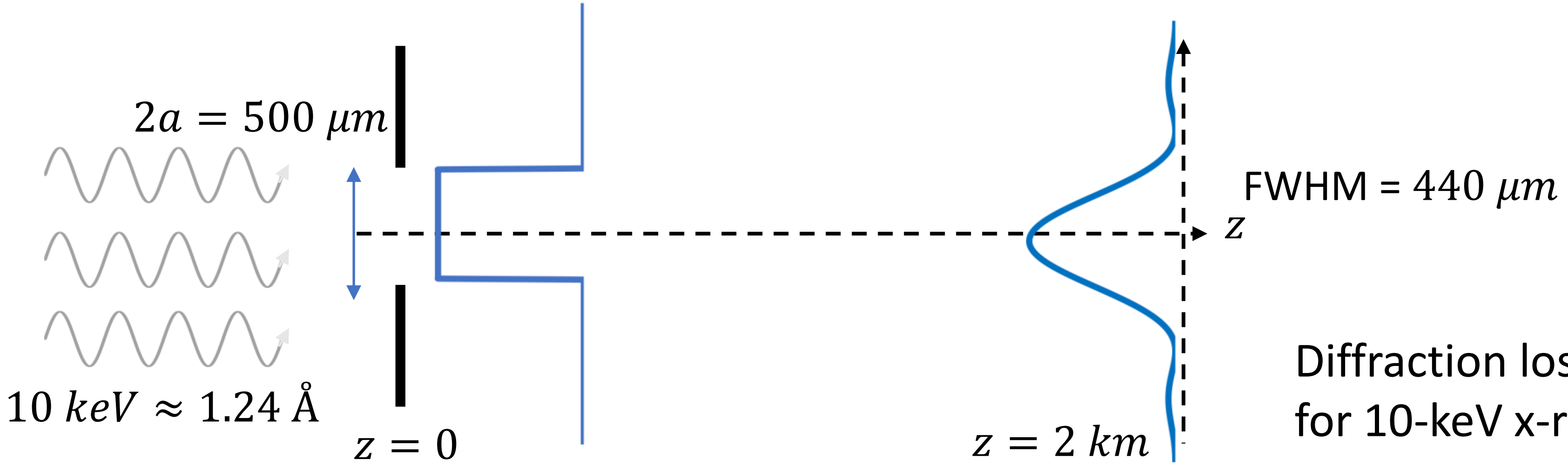

Diffraction loss is negligible for 10-keV x-rays over 2 km

The term diffraction is used to describe the propagation of light after passing through an aperture. The loss of power from the central cone (diffraction loss) depends on the Fresnel number, F. When F is less than 1, diffraction loss is significant.

Fresnel number $\quad F = a^2/\lambda L$

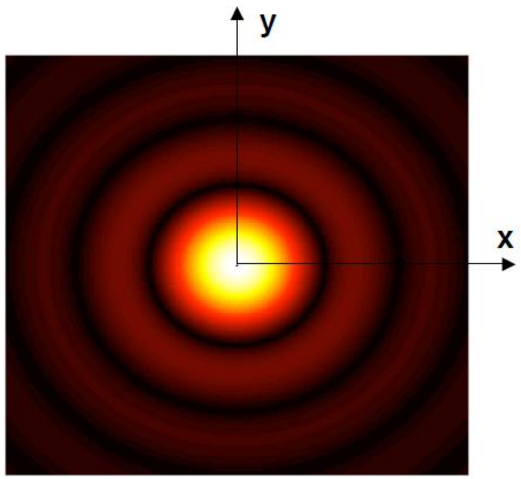

Airy disk diffraction pattern from a circular aperture

Young Double-Slit Diffraction

Diffraction can also be the interference from the wave propagation after interacting with multiple objects of the order of a few wavelengths of the light. For example, the double-slit diffraction, which creates bright and dark fringes at a distance L, is cause by the constructive and destructive interferences between two spherical waves emanating from the two slits.

$(d^2/\lambda \ll L)$

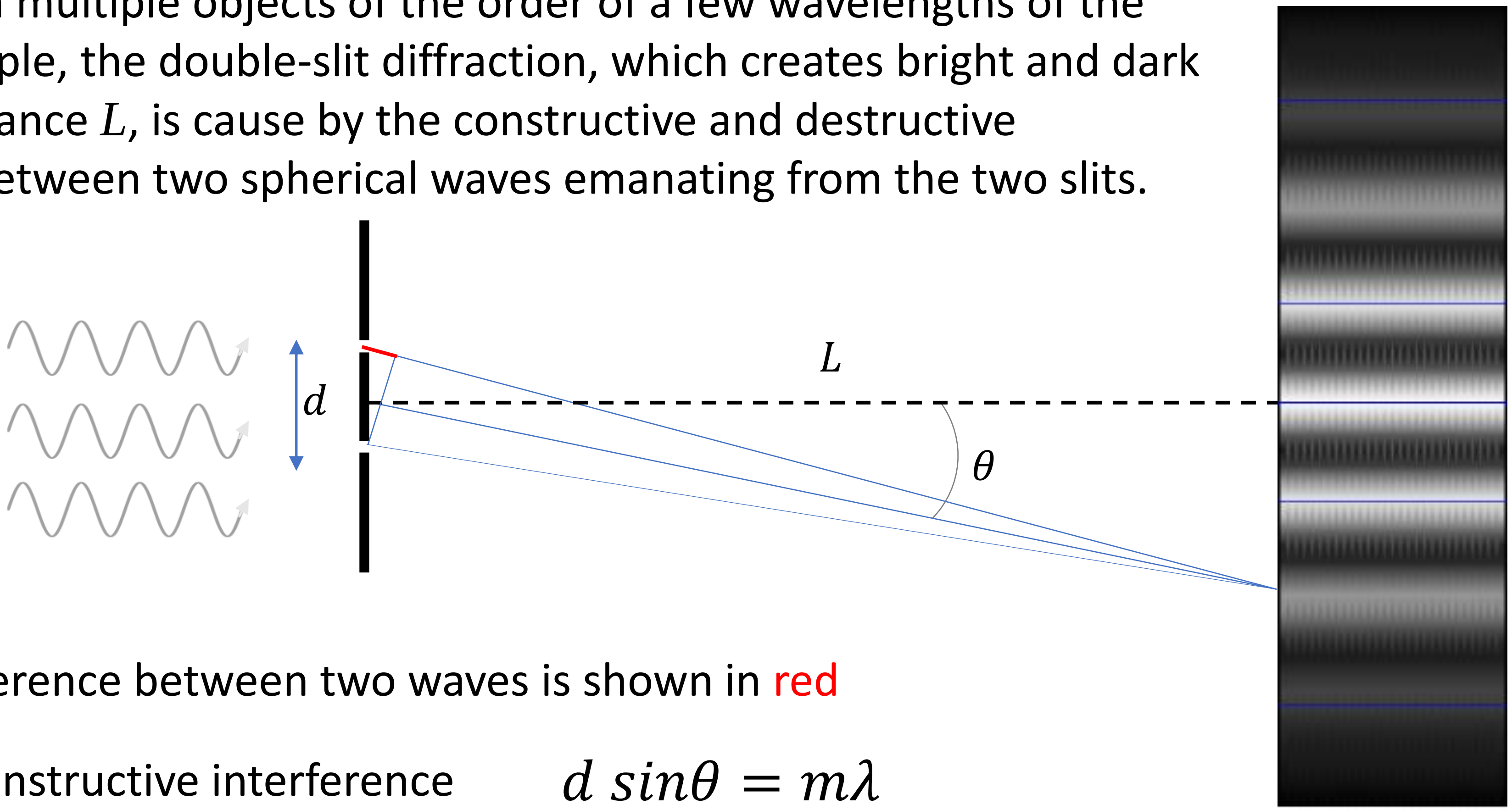

Path length difference between two waves is shown in red

Condition for constructive interference $$d\ sin\theta = m\lambda$$

SLAC NATIONAL ACCELERATOR LABORATORY

Los Alamos NATIONAL LABORATORY EST. 1943

Bragg Law of Diffraction

Diffracted waves

$$\boldsymbol{n\lambda = 2d\sin\theta_B}$$

Incident waves

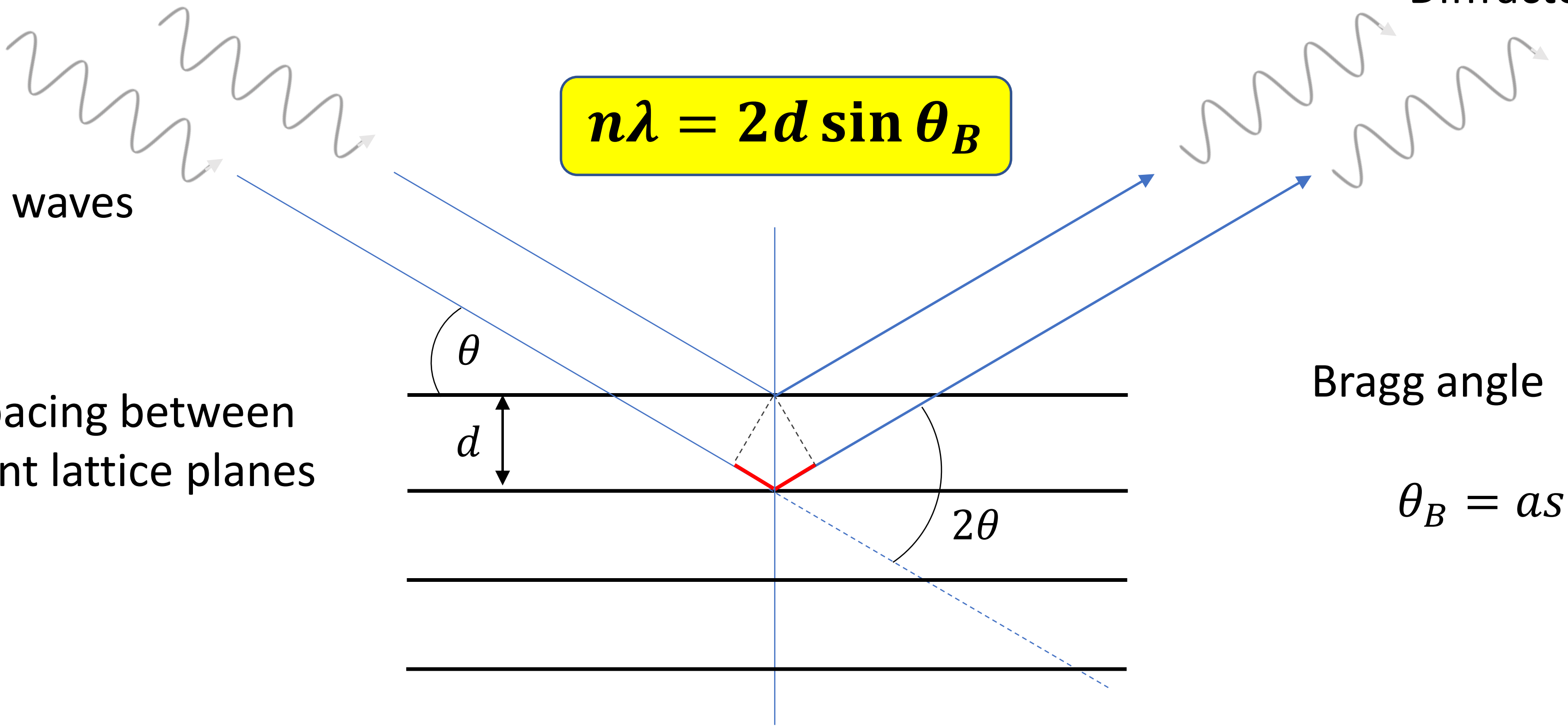

d = spacing between adjacent lattice planes

Bragg angle

$$\theta_B = asin\left(\frac{n\lambda}{2d}\right)$$

Bragg diffraction is an interference between two plane waves that are elastically scattered off lattice atoms with a spacing d between the adjacent lattice planes. The path length difference between two plane waves scattered off two adjacent lattice planes is shown in red. If the path length difference is a multiple of wavelengths, the scattered waves add constructively.

Bragg Crystals & Miller Indices

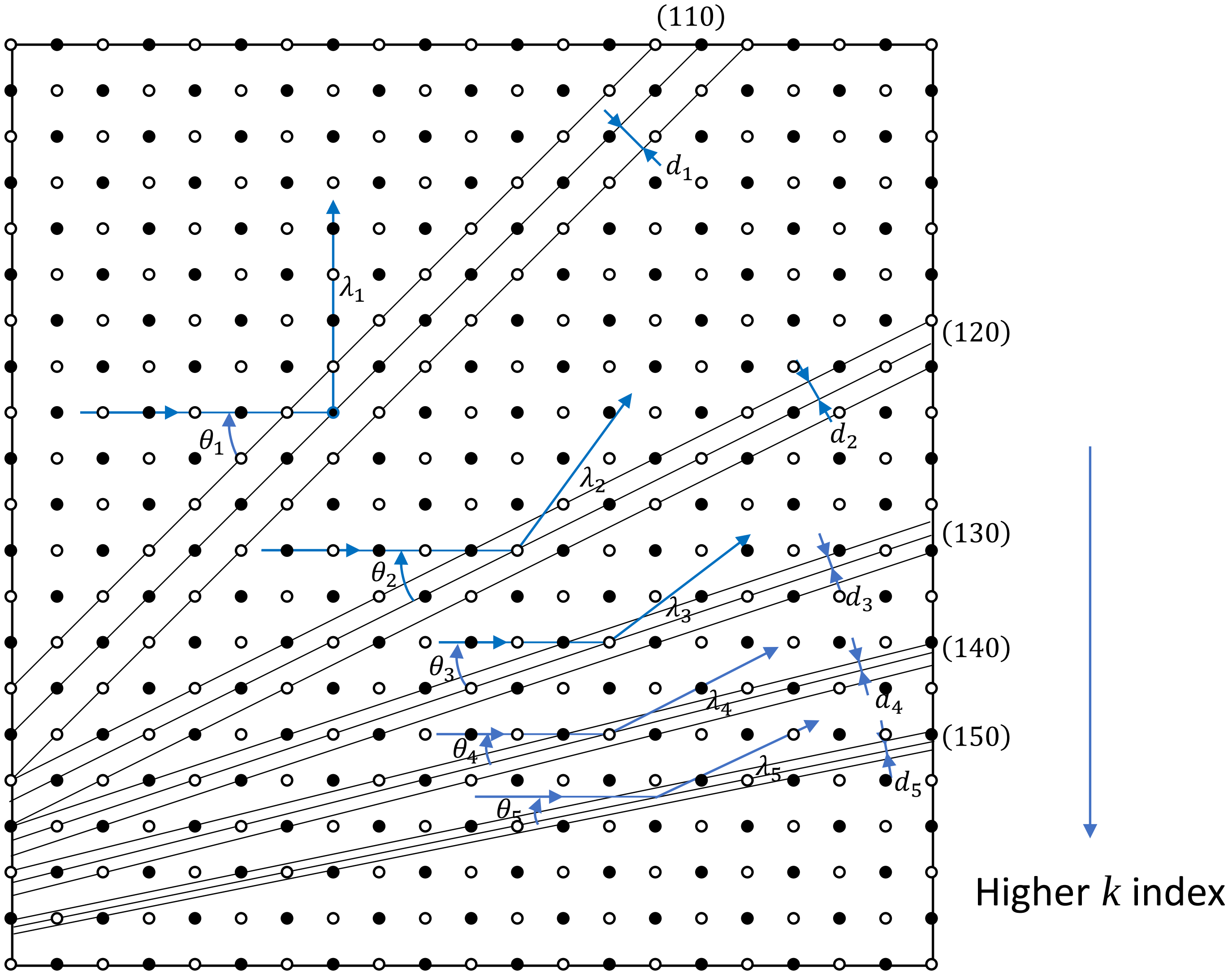

d spacing for different Miller indices

$$d_{hkl} = \frac{a}{\sqrt{h^2 + k^2 + l^2}}$$

a = atomic spacings

Example: Diamond a = 3.567 Å

Crystal hkl	d (Å)
Diamond (111)	2.0593
Diamond (220)	1.2611
Diamond (311)	1.5704
Diamond (400)	0.8917
Diamond (331)	0.8183

Courtesy of Andrew Aquila (SLAC)

Extinction Length

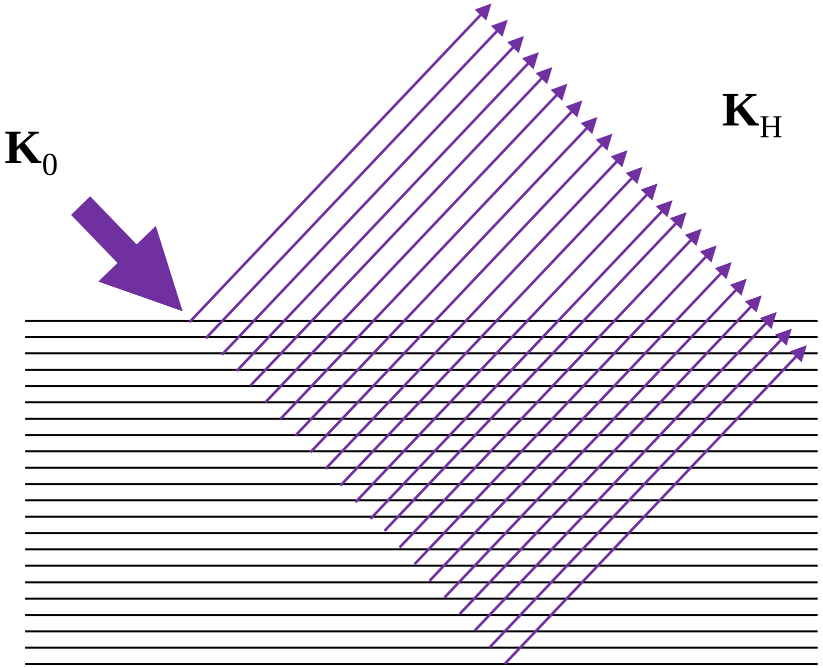

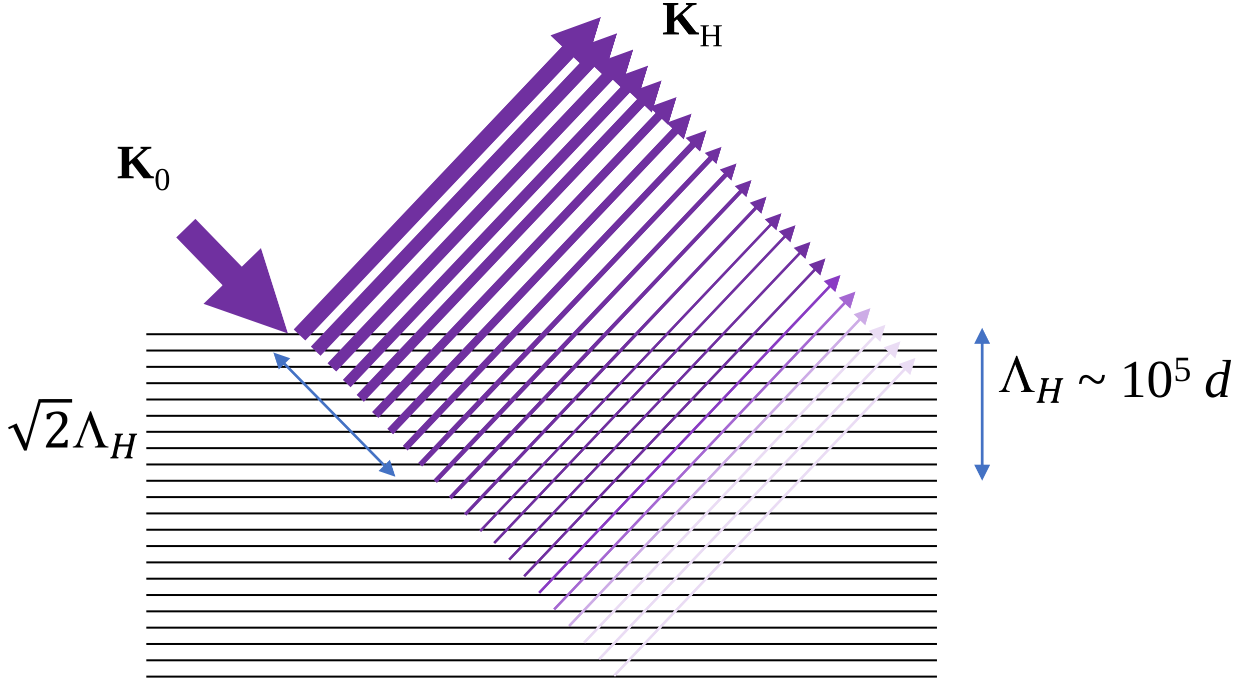

If the wave field penetrates an infinite distance into the crystal, all the diffracted rays would be parallel, i.e. the rocking curve would have zero width. In reality, most of the diffracted radiation is formed in a short depth in the crystal known as the extinction length. The finite "source size" gives rise to the rocking curve angular width $\Delta\theta$.

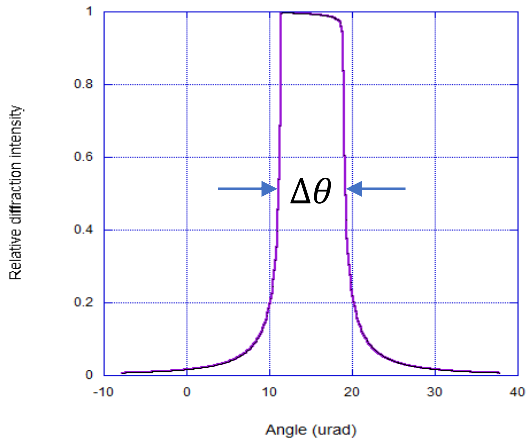

$$\Delta\theta = \frac{\lambda}{\pi\sqrt{2}\Lambda_H}$$

Rocking Curve & Darwin Width

The term “rocking curve” comes from a method in crystallography where the crystal is tilted by a small angle off the Bragg condition to produce a plot of diffracted x-ray intensity versus offset from the Bragg angle θ_B.

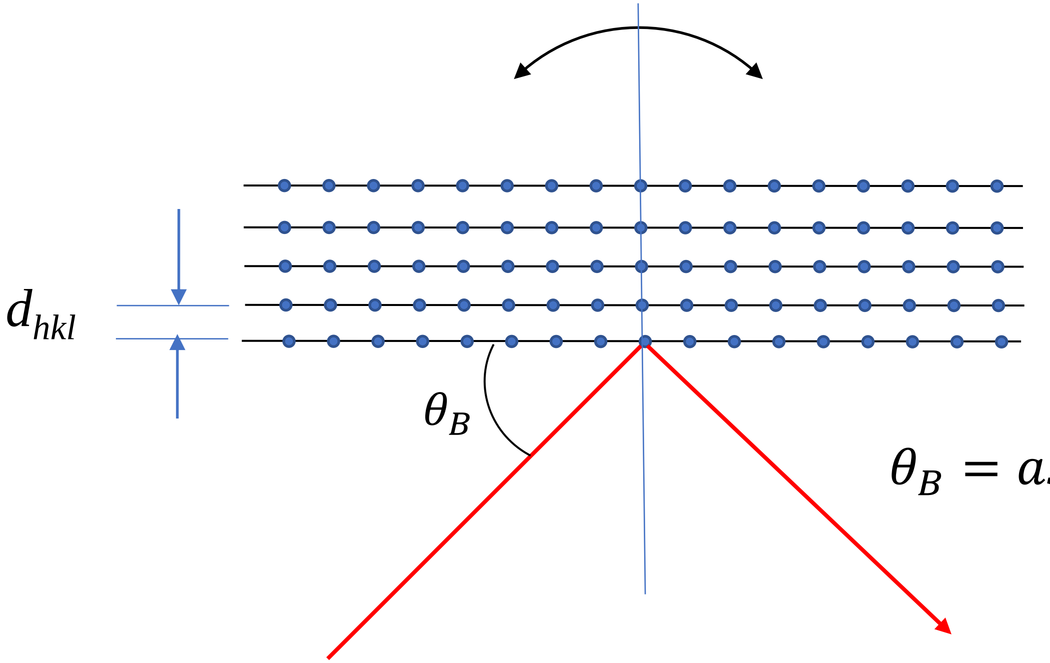

$$\theta_B = asin\left(\frac{n\lambda}{2d_{hkl}}\right)$$

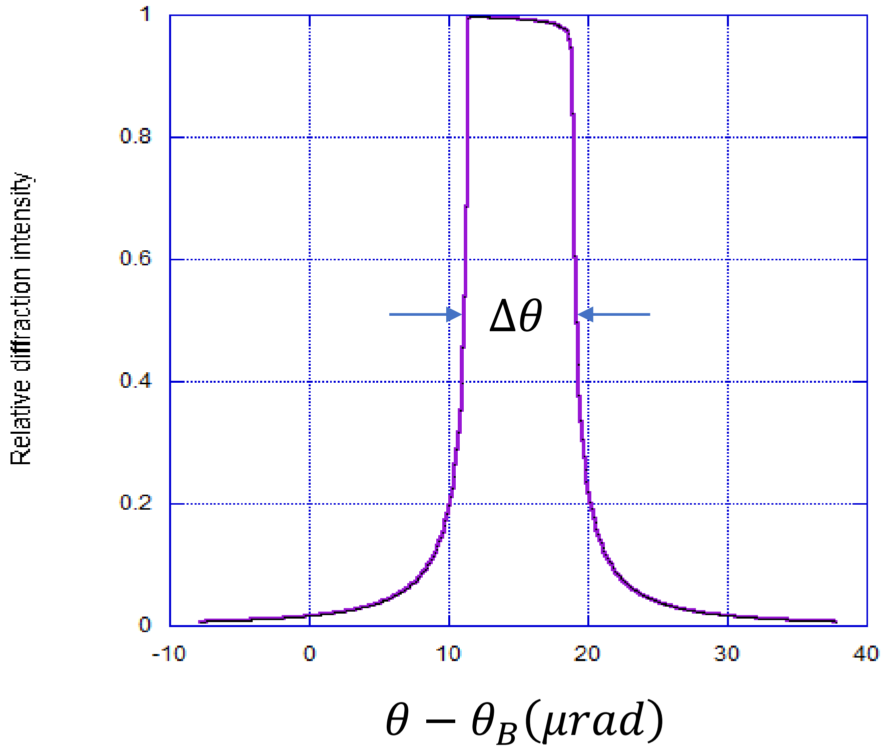

In symmetric Bragg diffraction, the incident and diffracted angles are the same as the Bragg angle θ_B.

Rocking Curve Angular Shift

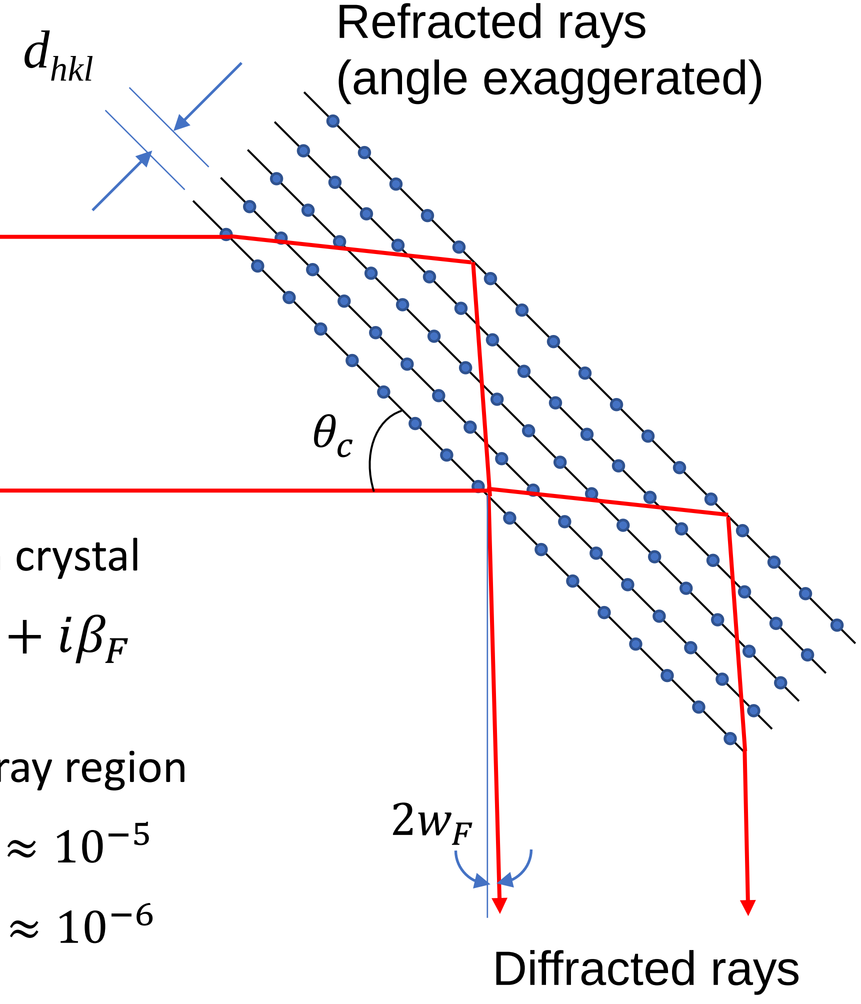

Refractive index in crystal

$$n_F = 1 - \delta_F + i\beta_F$$

Diamond in the x-ray region

Real part $\delta_F \approx 10^{-5}$

Imaginary part $\beta_F \approx 10^{-6}$

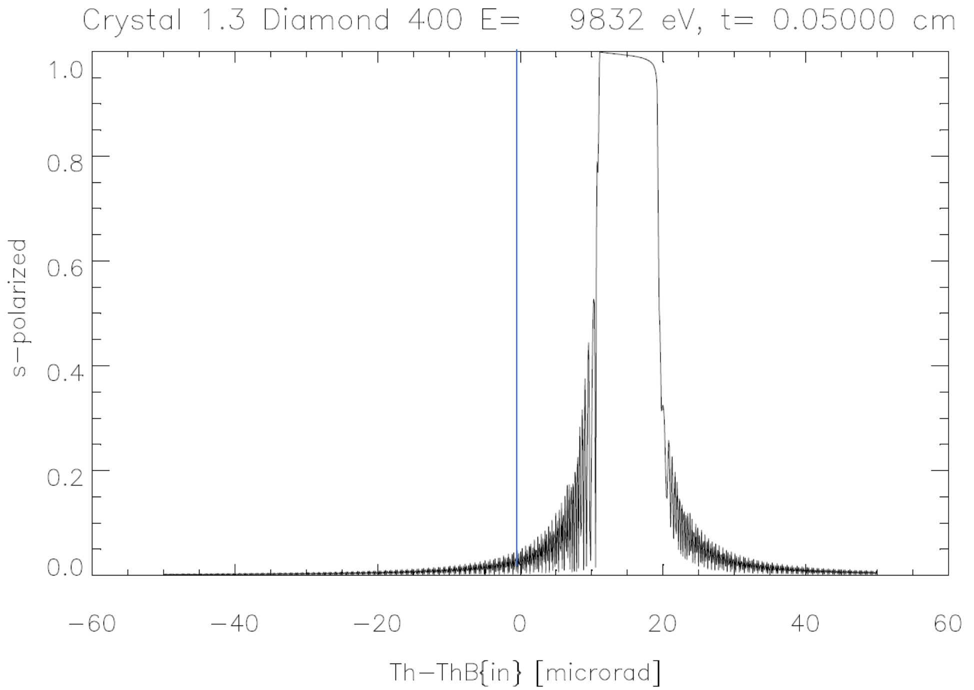

Corrected expression for diffracted angle

$$2d_{hkl} \sin\theta_c = \lambda(1 + w_F)$$

Symmetric Bragg Diffraction Crystals

Bragg Crystal	d (Å)	Photon energy at 45° (keV)	Darwin Width at 45° (μrad)	Energy Width (eV)	Extinction Length (μm)	Absorption Length (μm)
Silicon (111)	3.1355	2.796	133.2	0.37	1.5	2.525
Diamond (111)	2.0593	4.257	59.4	0.25	2.2	54.79
Diamond (220)	1.2611	6.952	19.4	0.14	4.14	220.7
Diamond (311)	1.0755	8.152	8.80	0.072	7.78	591.2
Diamond (400)	0.8918	9.831	7.56	0.074	7.5	1074.2
Diamond (331)	0.8183	10.713	4.26	0.046	12.24	1413.9
Diamond (422)	0.7281	12.041	4.41	0.053	10.51	2055.5

Energy width

$$\Delta\varepsilon = \epsilon\, \Delta\theta\, cot\theta_B$$

Extinction length is the depth over which the atoms contribute to Bragg diffraction

Λ_H = Extinction length

Absorption length is the length over which the radiation intensity decreases to 1/e of the incident intensity due to absorption

λ_A = Absorption length

Hard X-ray Self-Seeding

SASE Is Inherently Chaotic and Noisy

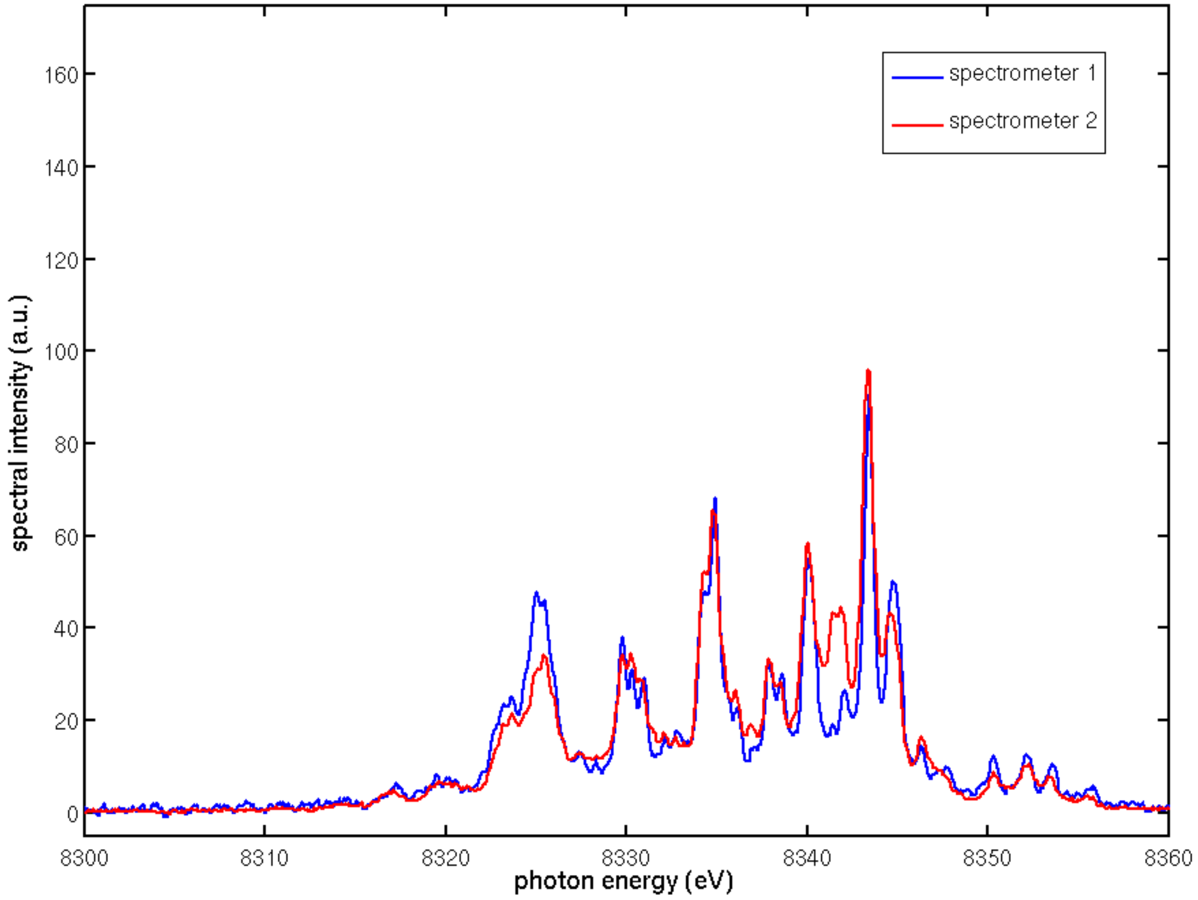

Fluctuations in the spectral (energy) domain of multiple SASE pulses from the LCLS x-ray FEL

SASE + Monochromator = Coherent Seed

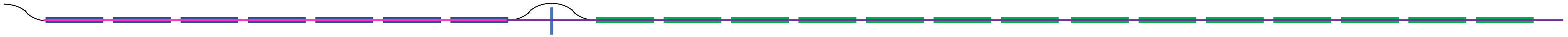

SASE is produced in Undulator Section 1

Coherent seed is amplified in Undulator Section 2

Monochromator filters SASE to produce coherent seed

Hard X-ray Self-Seeding (HXRSS)
Monochromator = thin Bragg crystal

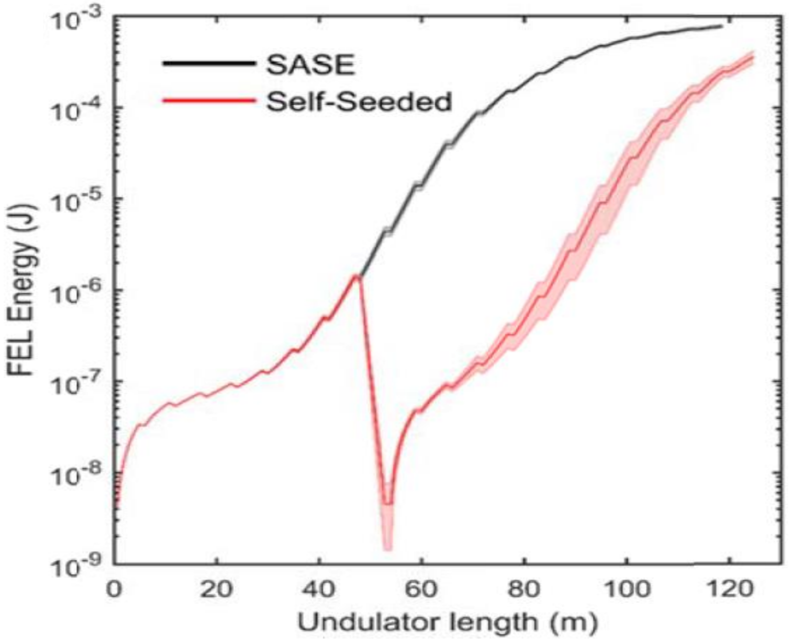

Soft X-ray Self-Seeding
Monochromator = a toroidal grating

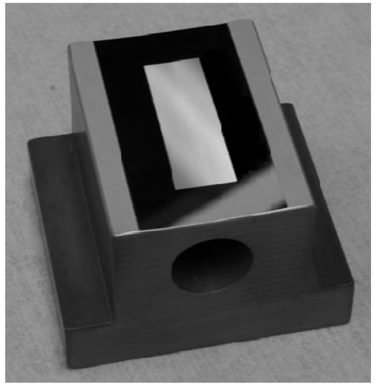

Hard X-ray Self-Seeding Experiments

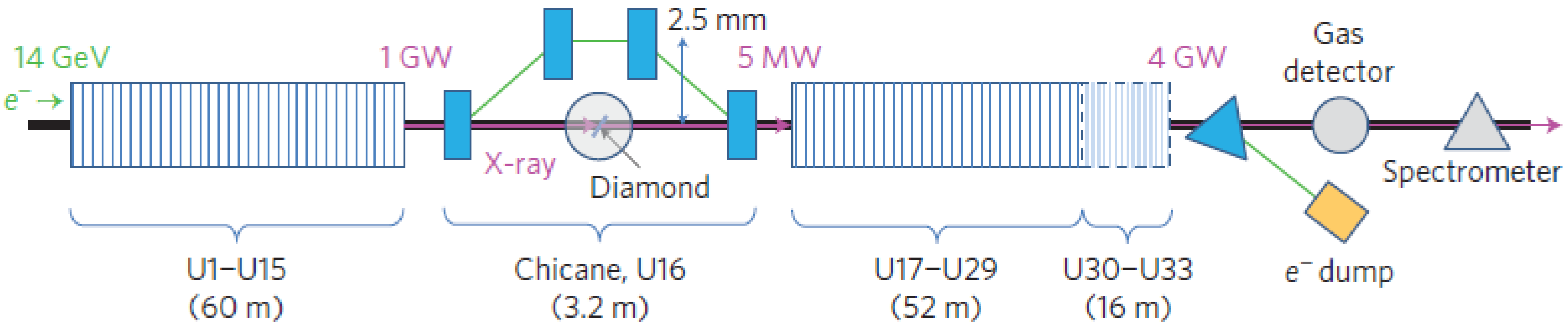

Chicane actions:
- wash out microbunching
- delay the electron bunch so it overlaps with one of the wake pulses
- offset the electron beam from the Bragg crystal

Diamond (400) : Photon energy: 7~10 keV

C(400), E_c=8.3 keV, η=0°, θ=56°

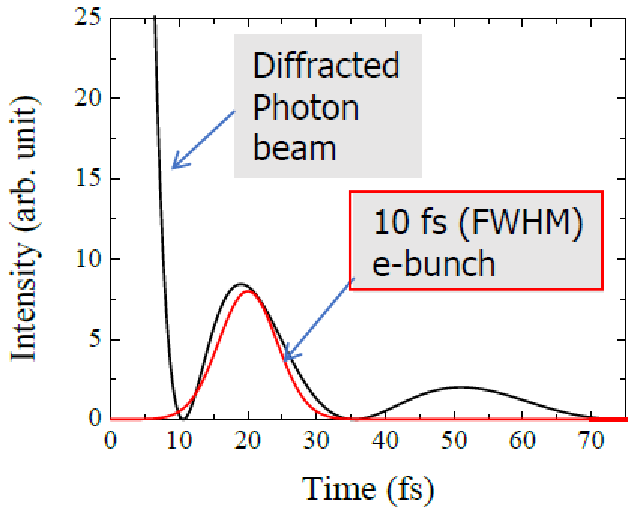

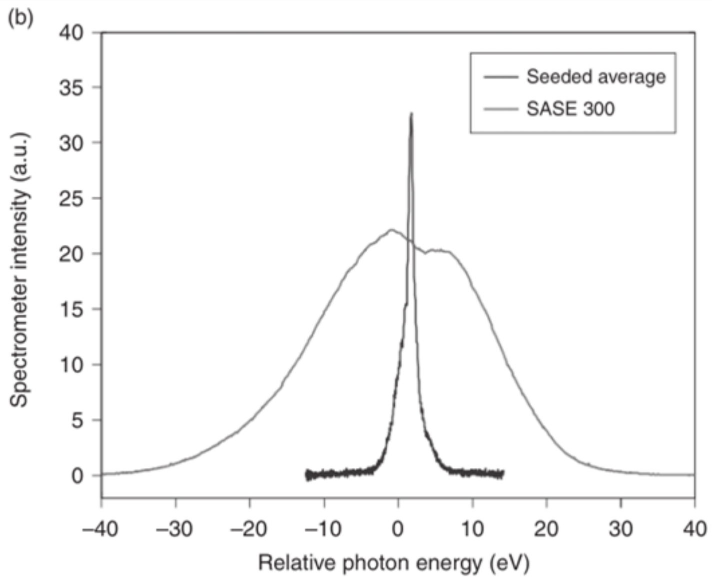

J. Amann et al., Nat. Photon. 6, 693 (2012)

HXRSS Spectral Brightness Enhancement

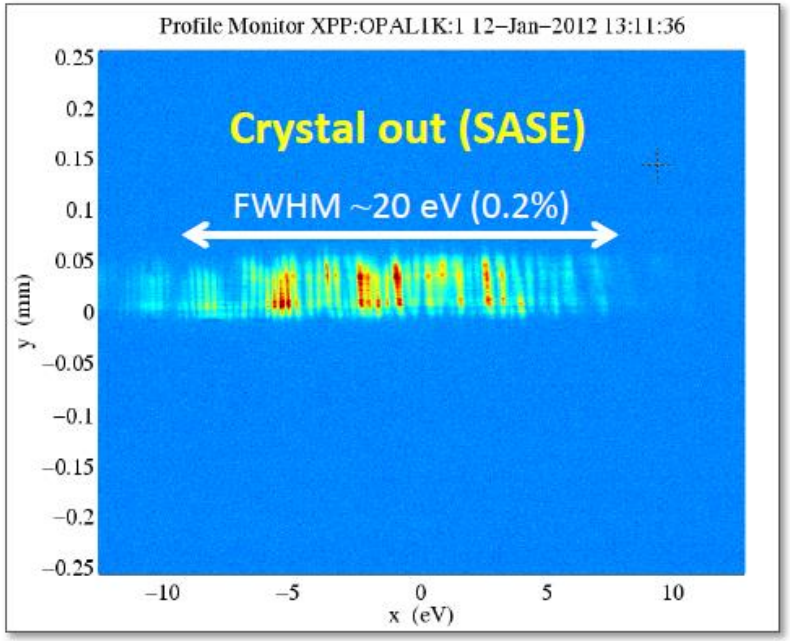

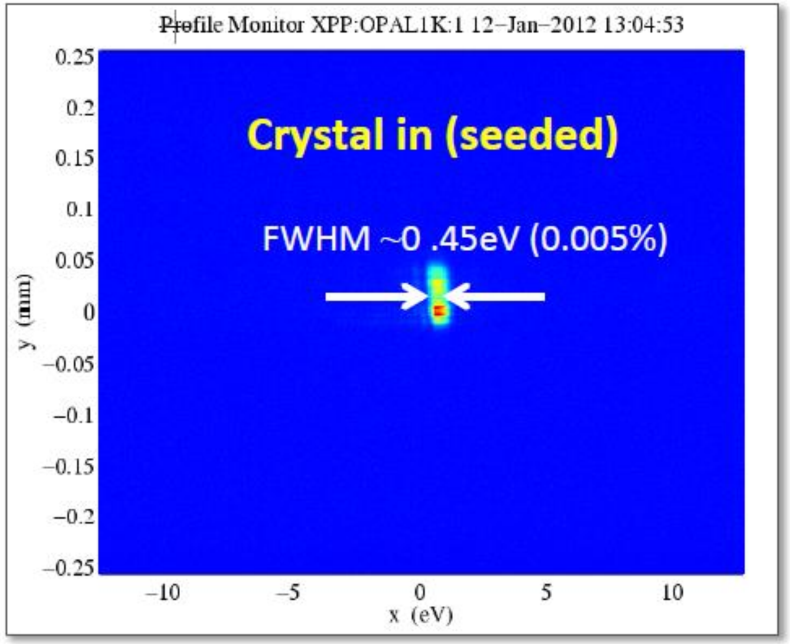

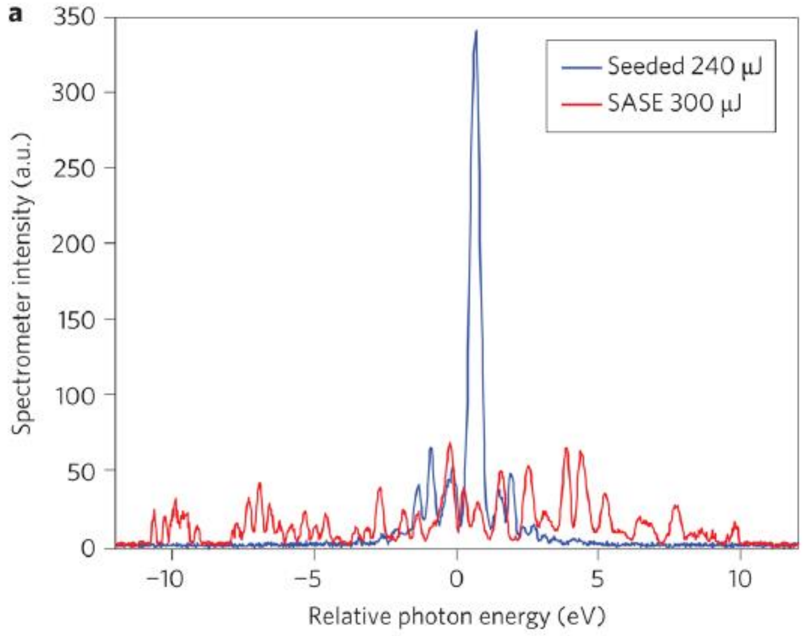

SASE relative BW

$$\frac{\Delta\omega}{\omega} \approx 1.5\rho \approx 2 \times 10^{-3}$$

HXRSS relative BW

$$\frac{\Delta\omega}{\omega} \approx 5 \times 10^{-5}$$

HXRSS brightness enhancement

$$\frac{\mathcal{B}_{SS}}{\mathcal{B}_{SASE}} \approx 30$$

Courtersy of the SLAC HXRSS Team

HXRSS reduces the SASE spectral width

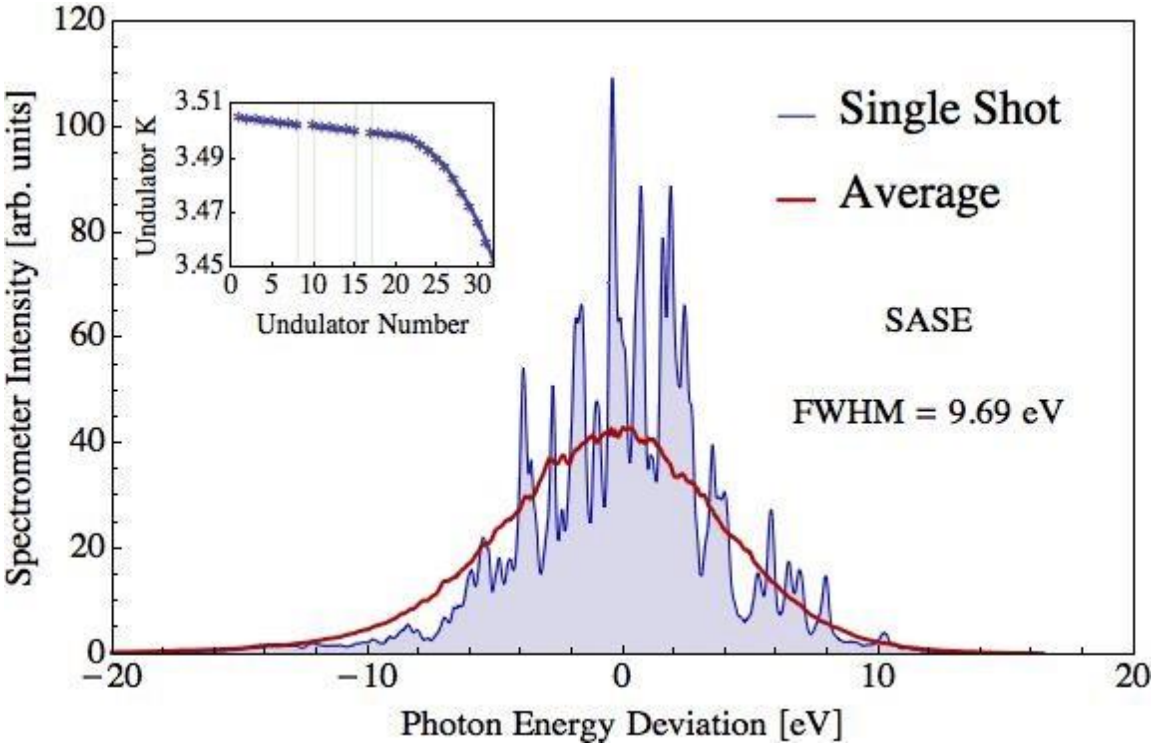

SASE spectra without self-seeding

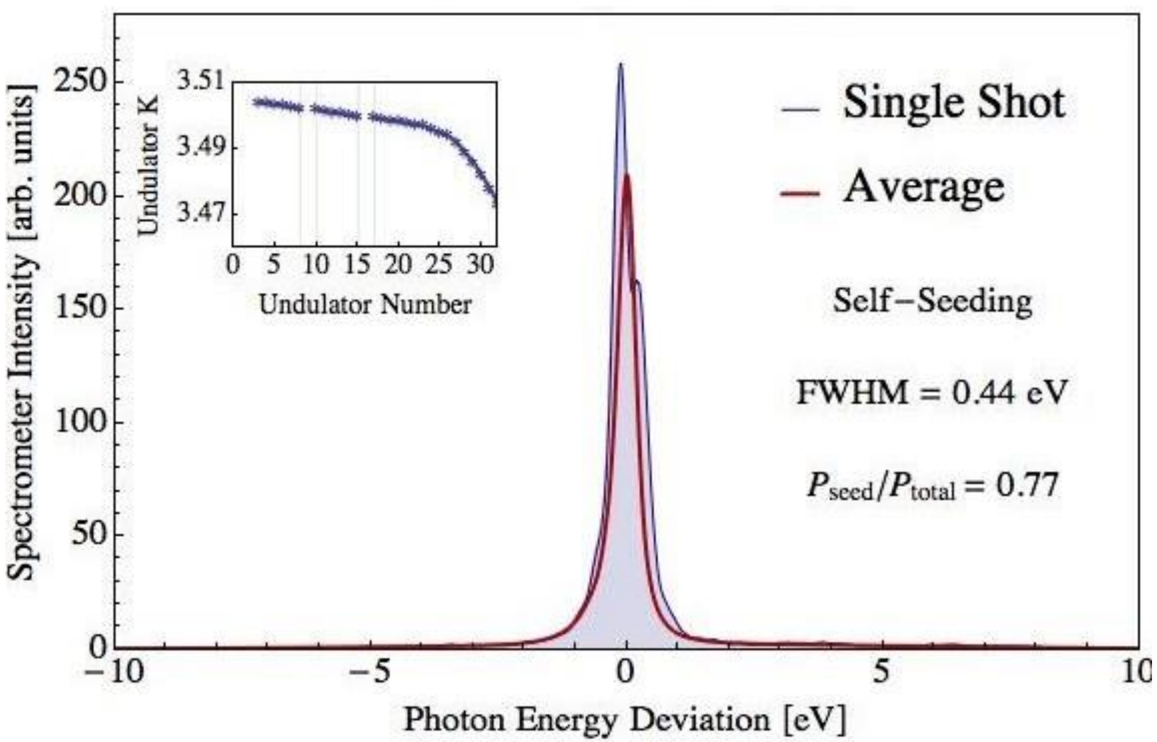

SASE spectra with self-seeding

C. Emma, UCLA Ph.D. Thesis (2017), https://escholarship.org/content/qt65p5d7h6/qt65p5d7h6.pdf

How does HXRSS generate the wake pulses?

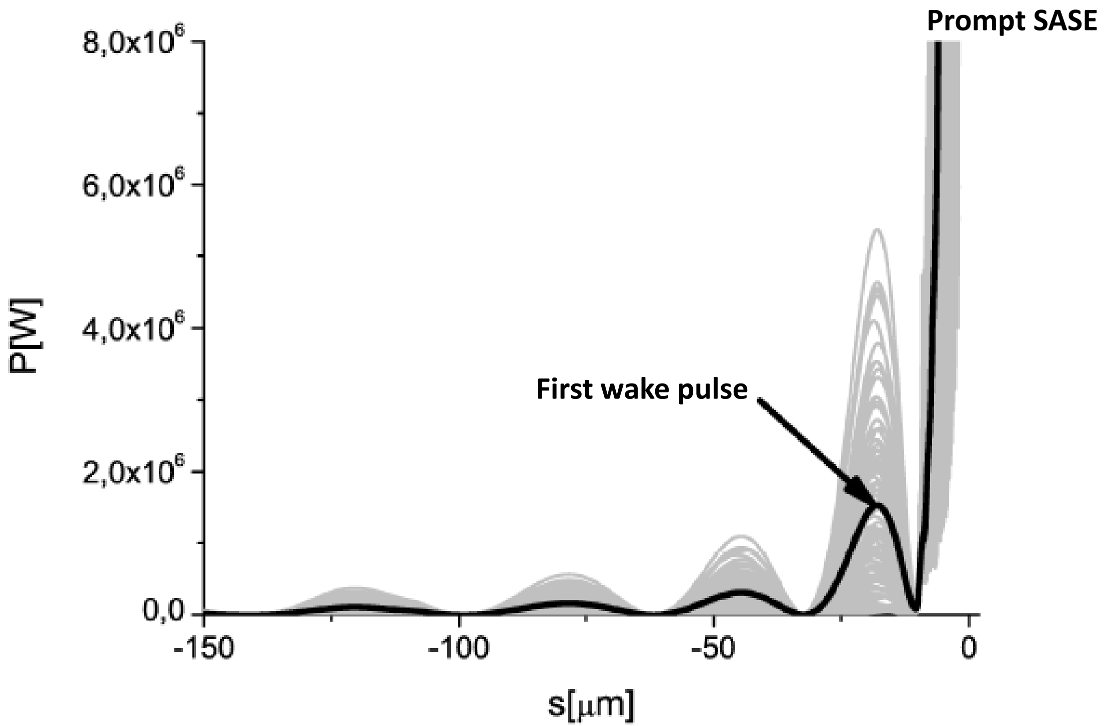

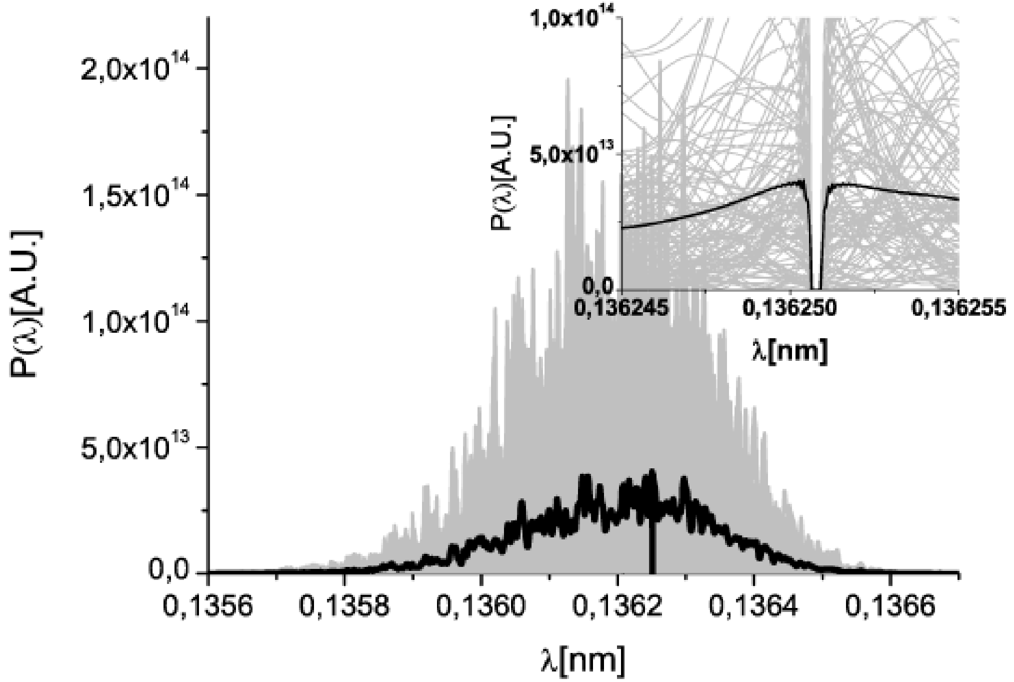

Bragg diffraction creates a spectral "notch" in the SASE spectrum. The Forward Bragg Diffraction (FBD) frequencies adjacent to the "notch" interfere constructively and destructively. In the time domain, this interference produces monochromatic wake pulses that follow the prompt SASE pulse.

L. Geloni et al., J. Mod. Opt. 58, 1391 (2011)

Bragg Spectral Response Functions

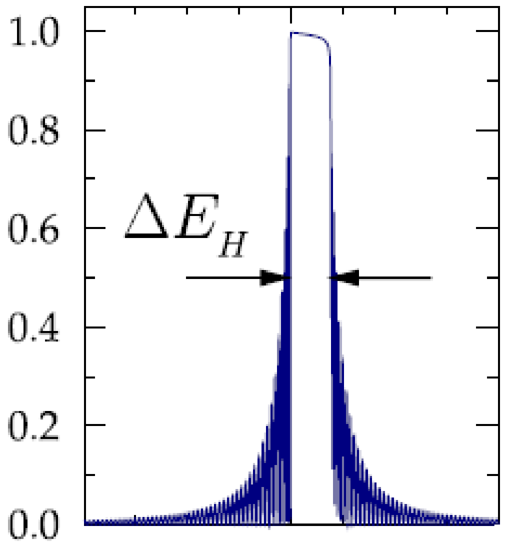

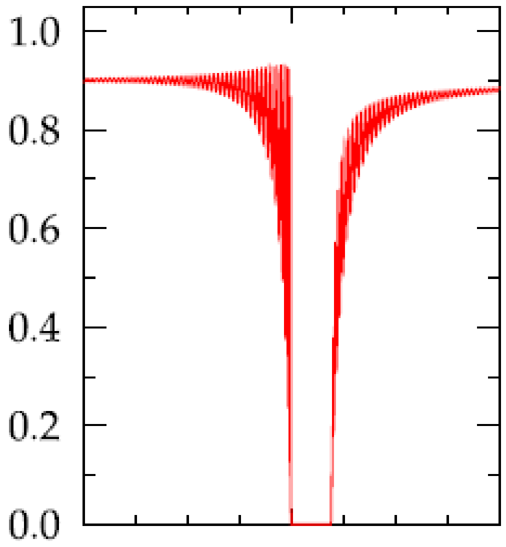

Reflected Bragg spectral response function

$$R_{0H} = R_1 R_2 \frac{1 - e^{i(\chi_1 - \chi_2)d}}{R_2 - R_1\, e^{i(\chi_1 - \chi_2)d}}$$

Forward Bragg spectral response function

$$R_{00} = e^{i\chi_1 d} \frac{R_2 - R_1}{R_2 - R_1\, e^{i(\chi_1 - \chi_2)d}}$$

Y. Shvyd'ko and R. Lindberg, Phys. Rev. ST Accel. Beam, 15, 100702 (2012)

Reflected (Backward) Bragg Diffraction

Bragg crystal

Incoming rays

Transmitted rays

Incoming radiation profile as a function of t

$$E_{in}(s) = E_0\, F(t)$$

Reflected Bragg diffraction

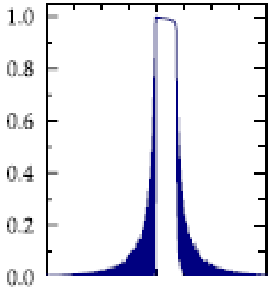

Incoming radiation spectrum as a function of ω

FT

$$\mathcal{F}(\omega) = \frac{1}{2\pi}\int_{-\infty}^{\infty} F(t)\, e^{-i\omega t} dt$$

Reflected Bragg spectrum as a function of ω

$$\mathcal{g}_{0H}(\omega) = R_{0H}(\omega)\mathcal{F}(\omega)$$

Reflected Bragg radiation profile as a function of t

$$E_{0H}(t) = E_0\, G_{0H}(t)$$

Inverse FT

$$G_{0H}(t) = \frac{1}{2\pi}\int_{-\infty}^{\infty} \mathcal{g}_{0H}(\omega)\, e^{i\omega t} d\omega$$

Forward Bragg Diffraction

Bragg crystal

Incoming rays

Forward Bragg diffraction

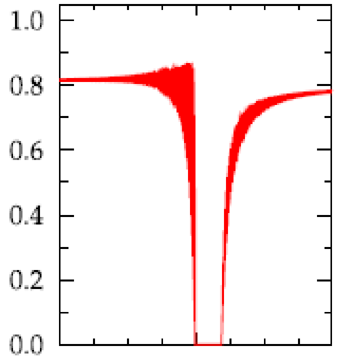

Incoming radiation profile as a function of t

$$E_{in}(s) = E_0 \, F(t)$$

FT

Incoming radiation spectrum as a function of ω

$$\mathcal{F}(\omega) = \frac{1}{2\pi}\int_{-\infty}^{\infty} F(t)\, e^{-i\omega t} dt$$

Forward Bragg spectrum as a function of ω

$$\mathcal{G}_{00}(\omega) = R_{00}(\omega)\mathcal{F}(\omega)$$

Inverse FT

Forward Bragg radiation profile as a function of t

$$E_{00}(t) = E_0 \, G_{00}(t)$$

$$G_{00}(t) = \frac{1}{2\pi}\int_{-\infty}^{\infty} \mathcal{G}_{00}(\omega)\, e^{i\omega t} d\omega$$

Monochromatic Wake Pulses

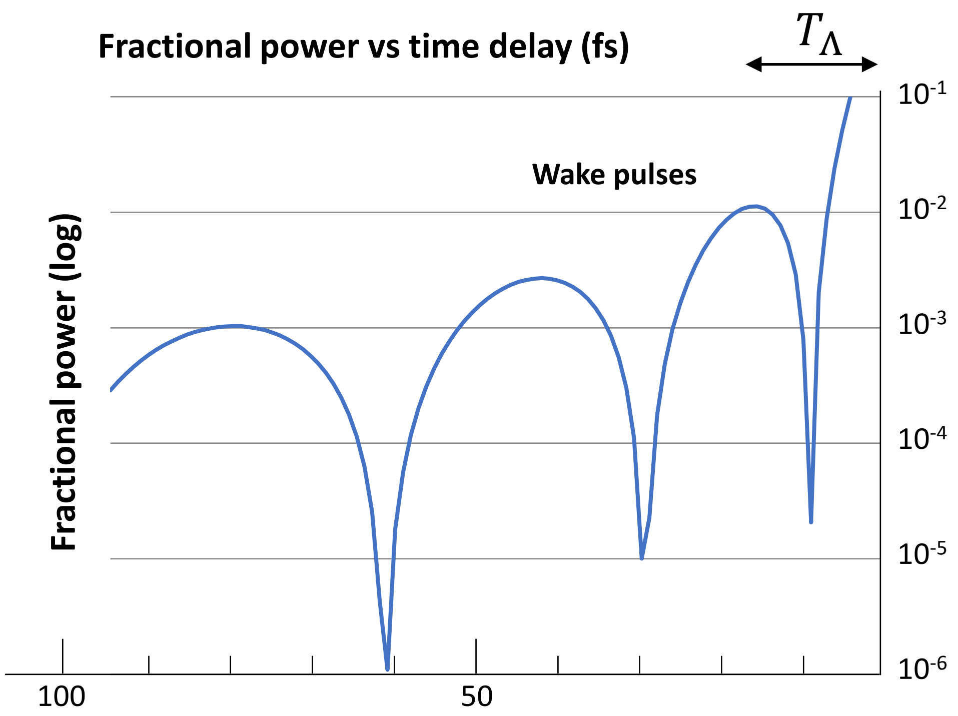

Central Energy $E_0 \approx \frac{1}{2}(E_{low} + E_{high})$

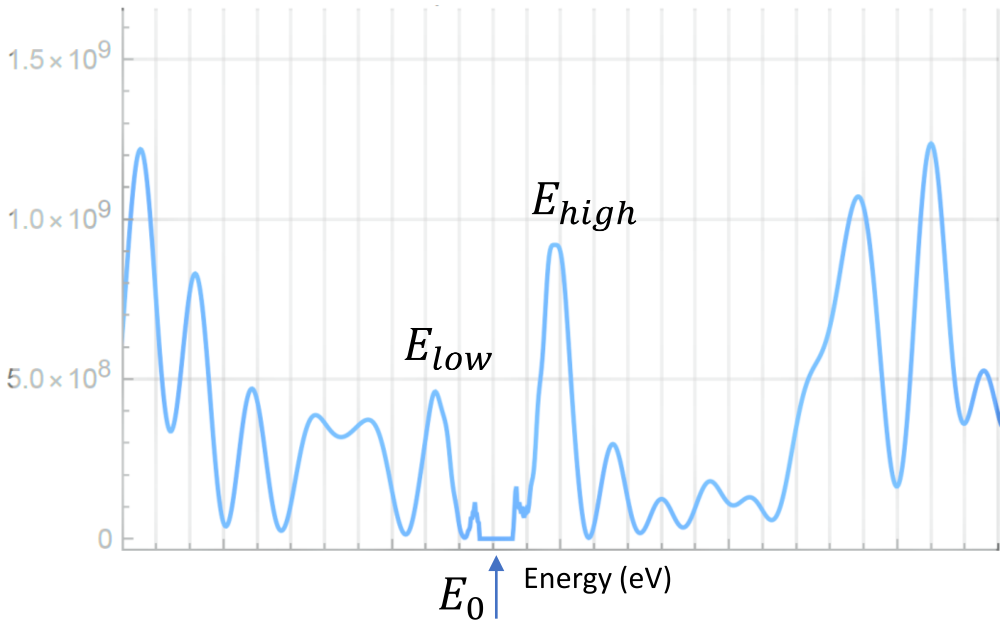

$$|G_{00}(t)|^2 \propto \left[\frac{1}{2T_0}\frac{J_1\left(\sqrt{\frac{t}{T_0}}\right)}{\sqrt{\frac{t}{T_0}}}\right]^2$$

First wake pulse delay

$$T_\Lambda = \frac{\Lambda_H}{2\pi\, c\, sin\theta_B}$$

Characteristic time

$$T_0 = \frac{\Lambda_H^2}{2\pi^2\, c\, d}$$

$\Lambda_H =$ Extinction length

$d =$ crystal thickness

Pathlength Delay & Offset in a Chicane

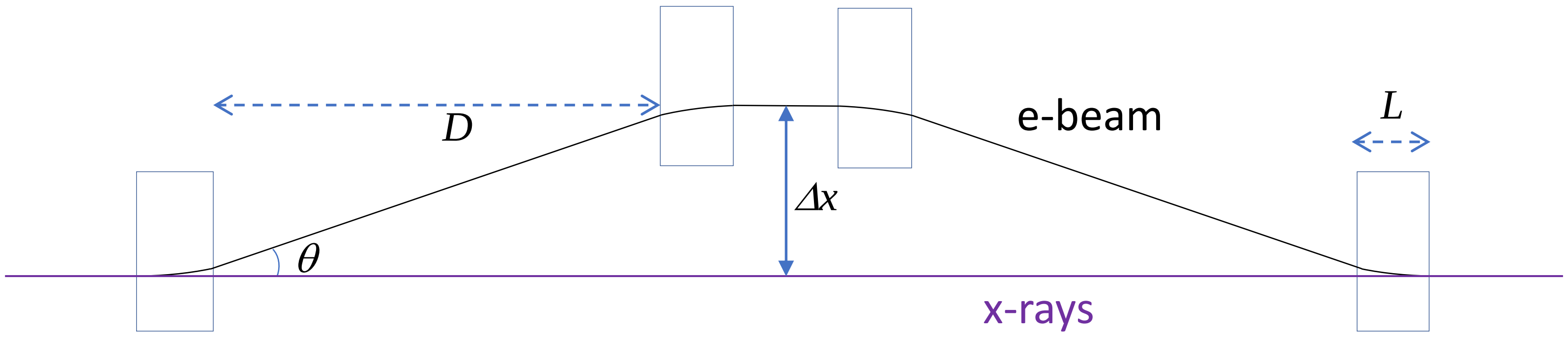

Difference between the electron and x-ray beam paths

$$\Delta L = \left(\frac{4}{3}L + 2D\right)\left(\frac{1}{cos\theta} - 1\right)$$

Chicane delay using small-angle approximation

$$\Delta L \approx \left(\frac{2}{3}L + D\right)\theta^2$$

Electron beam delay

$$\Delta t = \frac{\Delta L}{c} \qquad c = 0.3\ \mu m/fs$$

Shot-to-shot Pulse Energy Fluctuations

Relative pulse energy fluctuation scales with $\sqrt{1/M}$

$$\frac{\sigma_W}{W} = \frac{\langle W - \langle W \rangle \rangle}{\langle W \rangle} \propto \sqrt{1/M}$$

where M = number of modes.

SASE $M \approx 160$ $\quad \frac{\sigma_W}{W} \approx 8\%$

HXRSS $M \approx 12$ $\quad \frac{\sigma_W}{W} \approx 30\%$

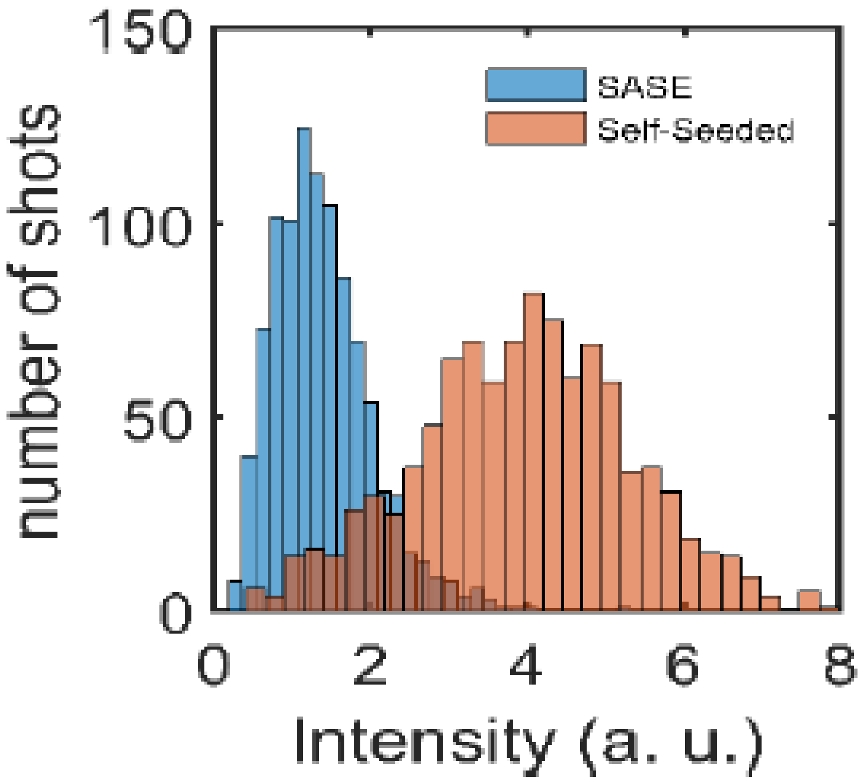

With the smaller M, HXRSS has much larger shot-to-shot pulse energy fluctuations than SASE

C.K. Min et al., J. Synchrotron Rad. 26, 1101 (2019)

HXR Self-Seeding with Channel-cut Crystals

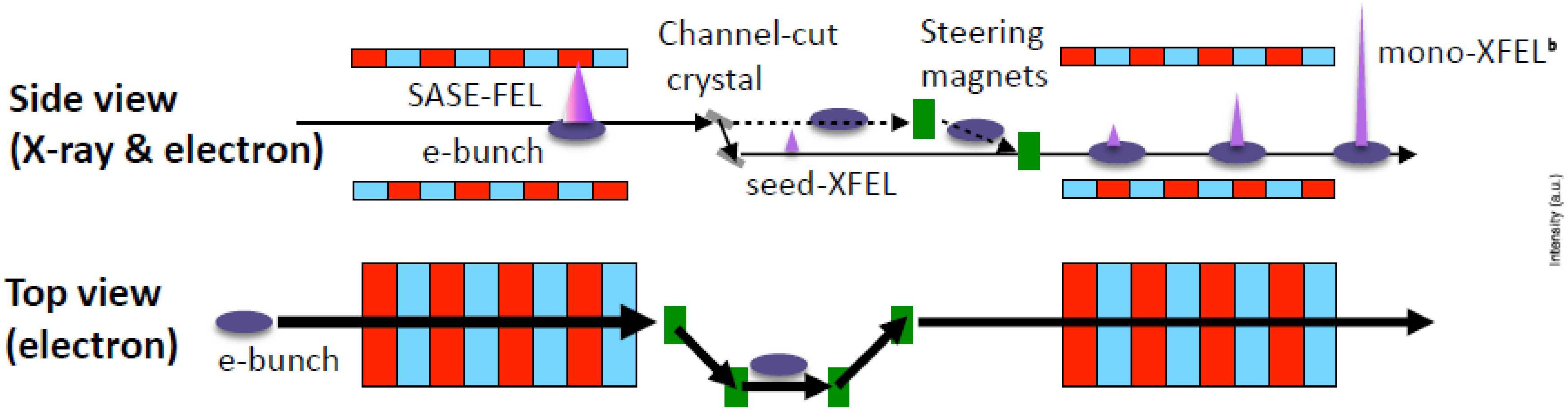

Magnetic chicane

J. Feldhaus, *Opt. Lett* (1997).
I. Inoue *et al.*, *Nat. Photon.* (2019)

Channel-cut crystal

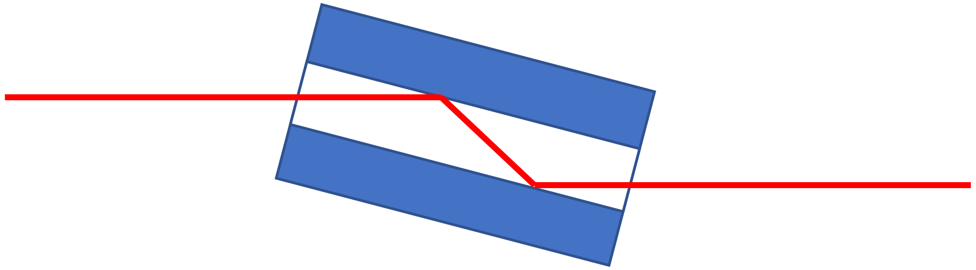

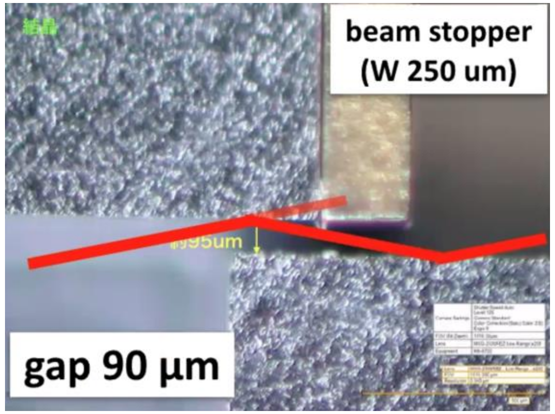

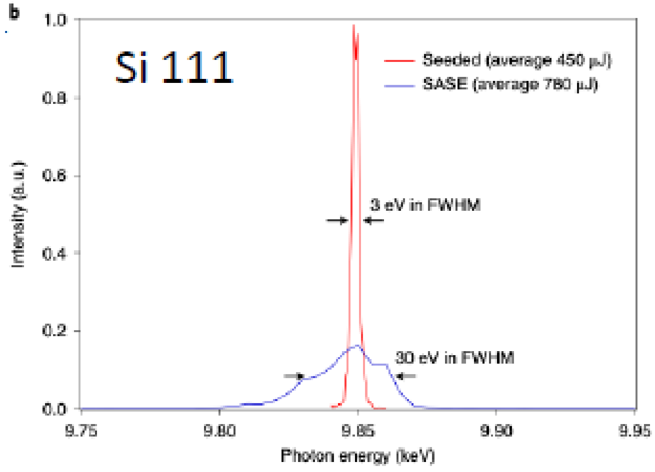

I. Inoue et al., Nat. Photon. 13, 319 (2019)

SASE Self-Seeding Photon Energy Coverage

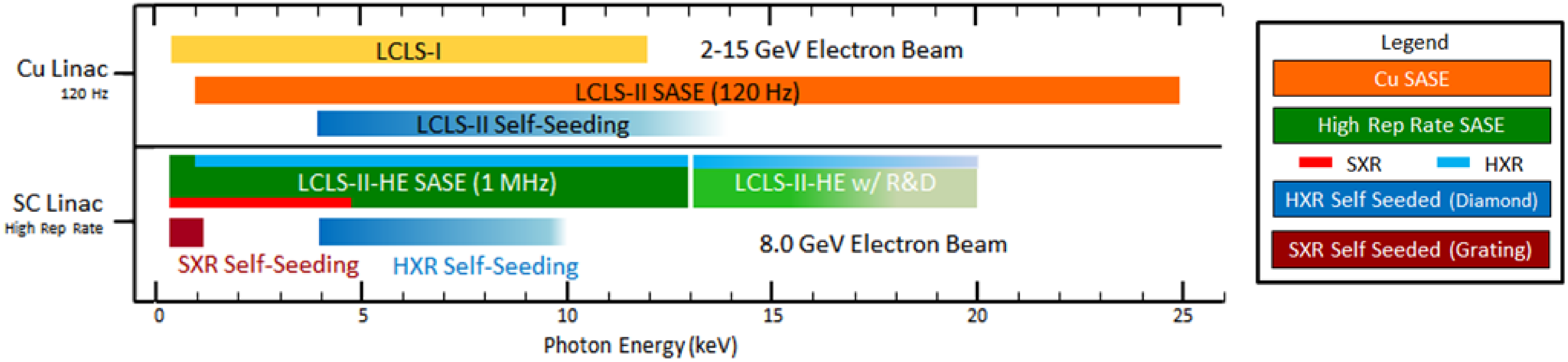

Gap in the Self-Seeding energy coverage between 1 and 4 keV is due to:

- Material absorption (very strong at low photon energies)
- Reduced reflectivity of gratings

Soft X-ray Self-Seeding

Soft X-ray Self-Seeding at LCLS

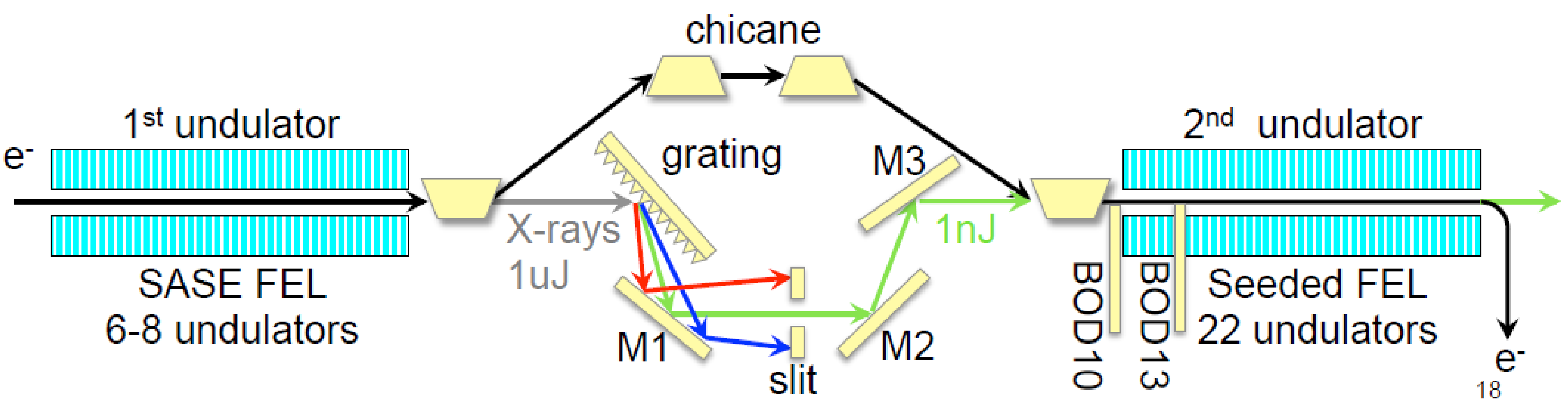

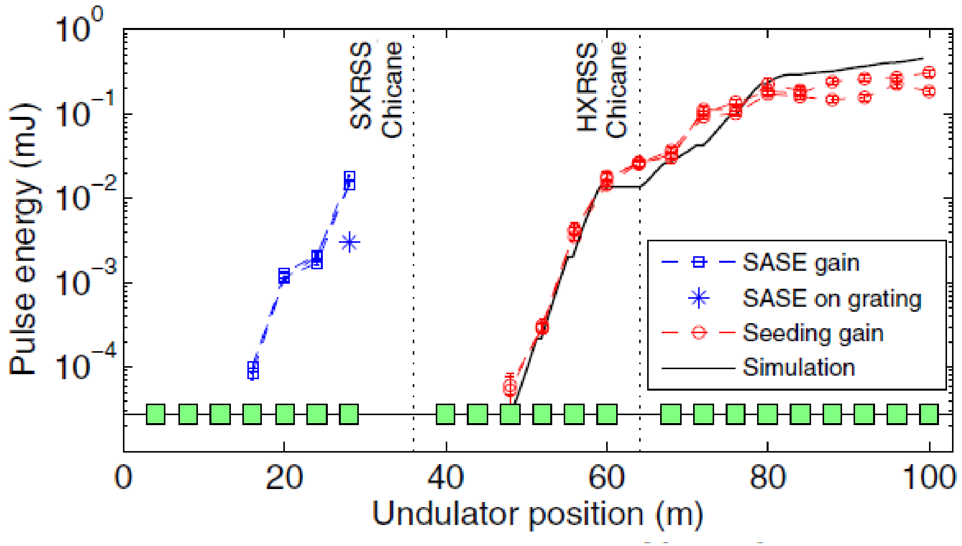

Seeding ~4x brighter than SASE

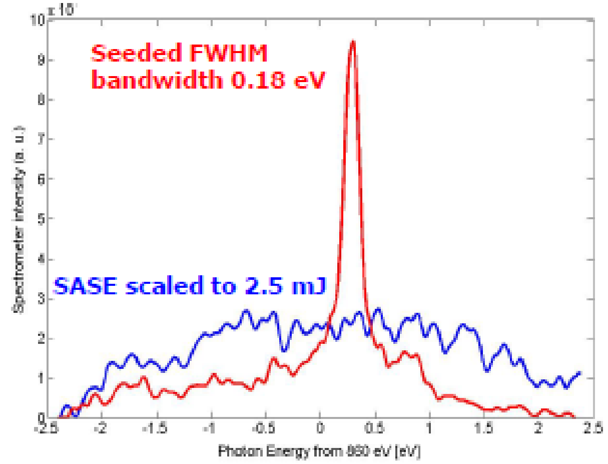

1.5-2 kA, 75-100 fs, 1-10uJ incident on grating

D. Ratner *et al.* Phys. Rev. Lett. **114**, 054801

SXRSS Diffraction Grating

Grating equation

$$\boxed{n\lambda = d(\sin\alpha - \sin\beta)}$$

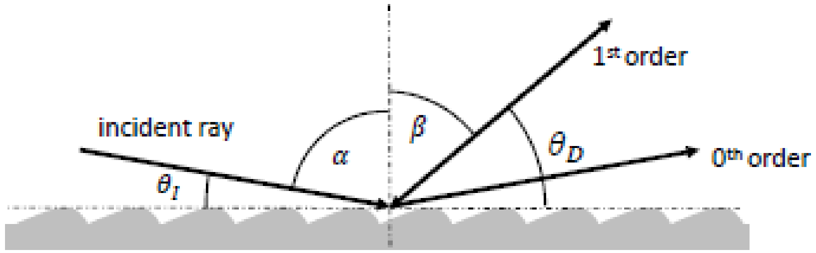

Parameter	*Symbol*	*Value*	*Unit*
Line spacing	d	0.4452	μm
Linear coeff	$\Delta d/\Delta x$	$-6.621\text{x}10^{-7}$	
Groove height	h	15.6	nm
Grating efficiency @0.2 – 1.3 keV	η_{Grating}	3.77 - 0.58	%

For LCLS SXRSS, the incident angle α is fixed at 89°

The exit angle β depends on the x-ray energy

Tuning x-ray energy by rotating M1 mirror about the pivot

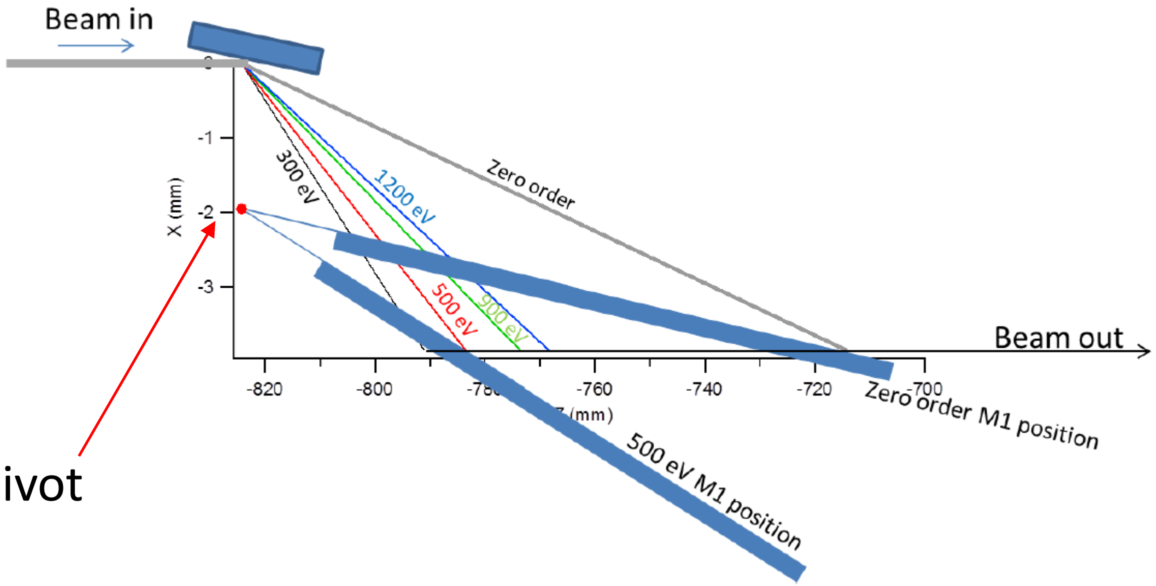

Focusing Property of the Toroidal Grating

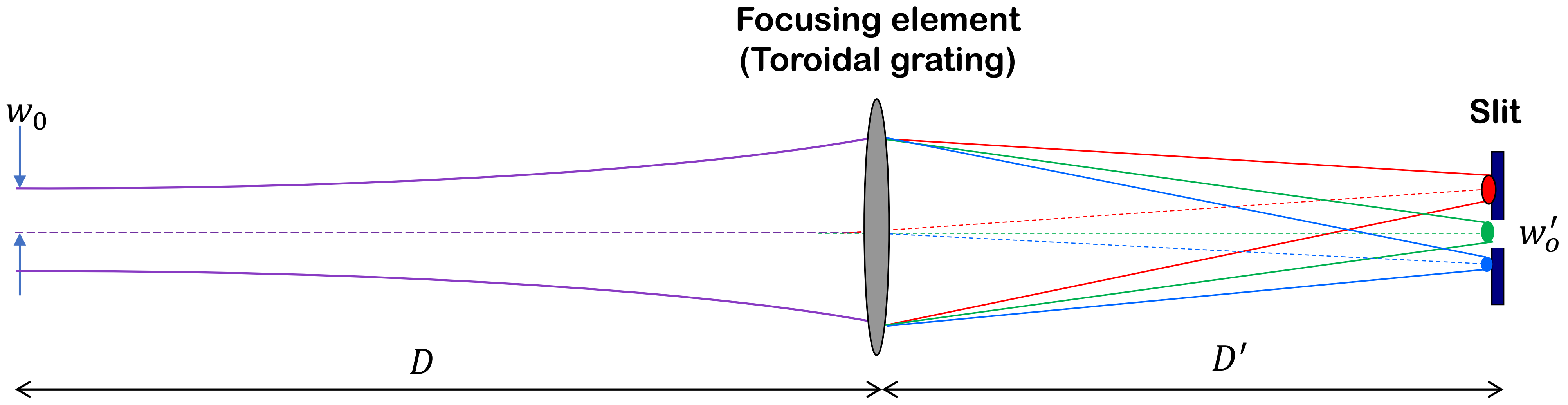

The toroidal grating focuses the x-ray beam on the slit and disperses different x-ray energies along the horizontal axis. The focusing property is energy dependent. At low x-ray energy, the SASE spectral width and w_o' are large, so the slit used to transmit the monochromatic seed with 1% bandwidth is also large. Therefore, the slit must have variable widths.

Photon energy	Vertical spot size (FWHM)	Horizontal spot size (1% SASE bandwidth)
(eV)	(μm)	(μm)
300	96	679
400	88	590
700	73	403
1000	65	284

SXRSS Delays (pathlength divided by c)

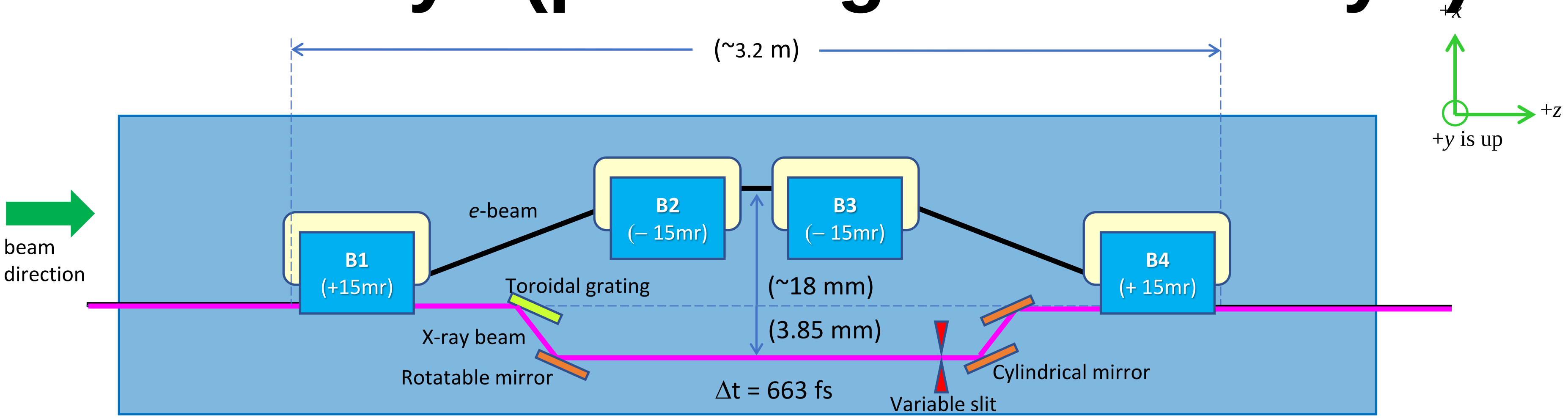

Unlike HXRSS, SXRSS must overlap the electron bunch with the main X-ray pulse

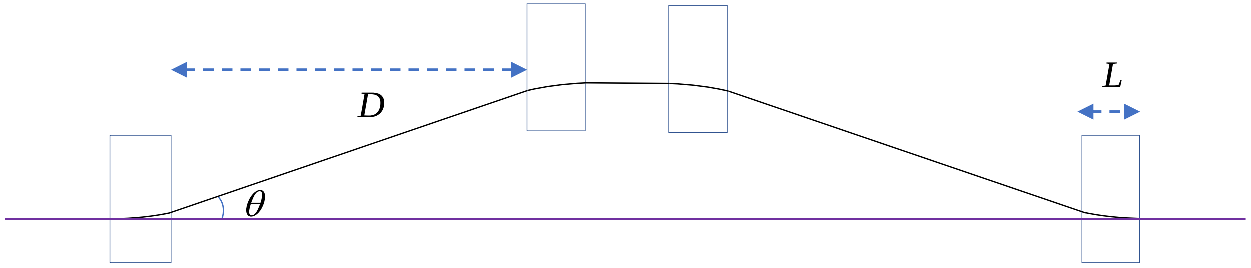

Electron extra pathlength $\Delta L_b = \left(\frac{2}{3}L + D\right)\theta^2$

X-ray extra pathlength $\Delta L_r = 2\Delta x \cdot cot\phi$

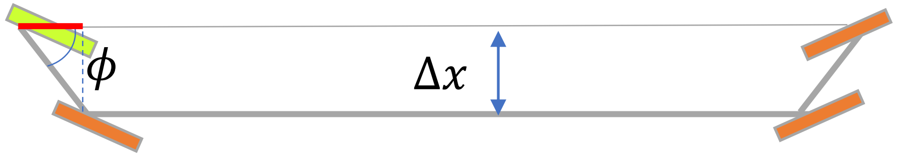

SXRSS Performance at 1 keV

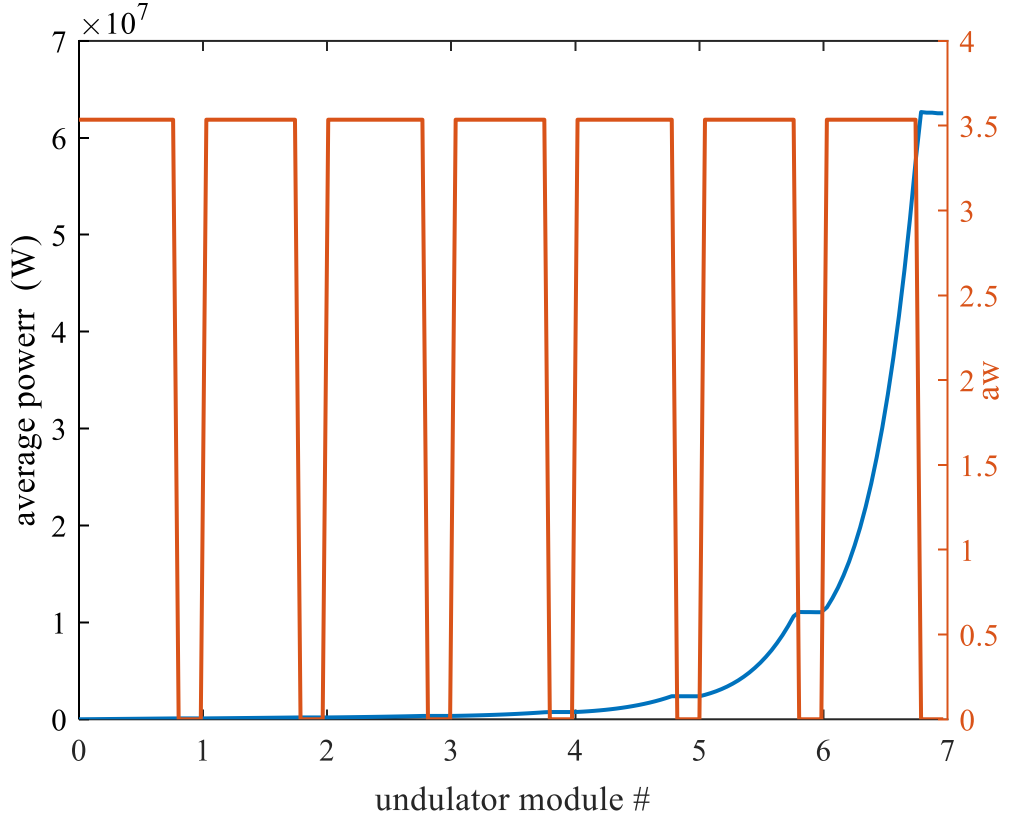

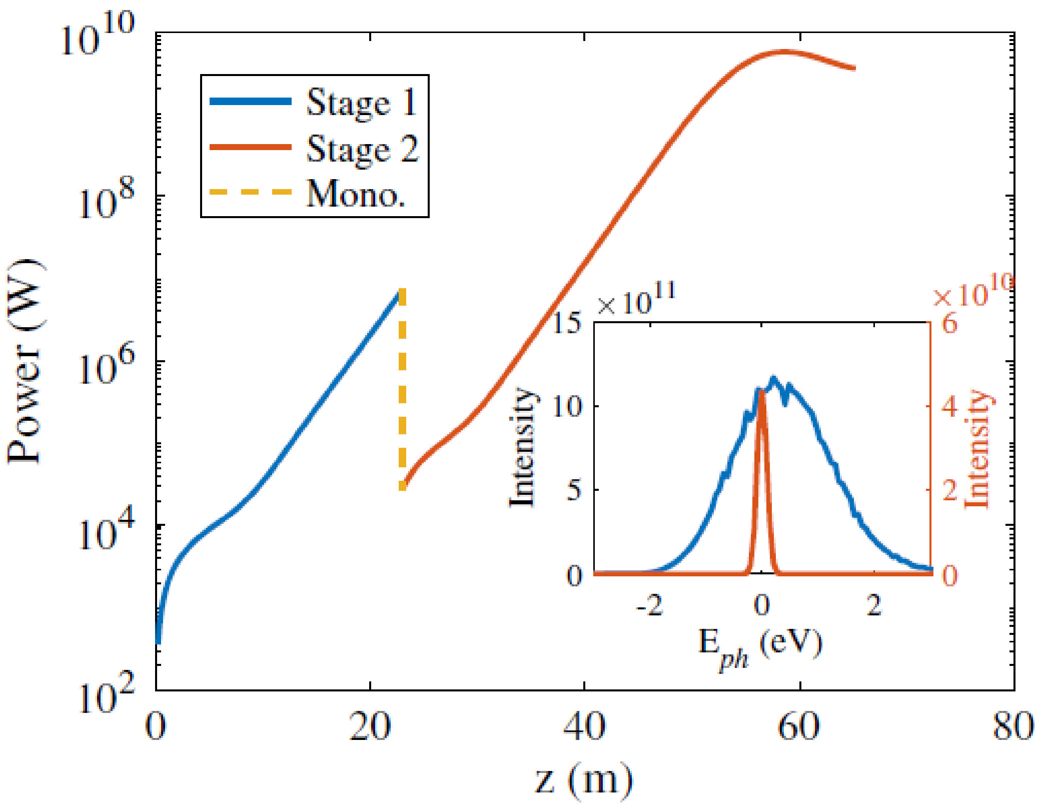

Max. seed power is 20 kW
(limited by grating damage)

Final SXRSS power is 8 GW

Regenerative Amplifier FEL

SASE, RAFEL and XFELO

	SASE	XRAFEL	XFELO
Peak Power	~10 GW	~50 GW	~100 MW
Average power	~100 W (at ~1 MHz)	10 W (at 10 kHz)	20 W (at ~1 MHz)
Spectral bandwidth	~10 eV	~0.1 eV	~1 meV
Pulse length	~ 1 – 100 fs	~ 20 fs	~ 1 ps
Stability	Poor	Excellent	Excellent
Longitudinal coherence	Poor	Excellent	Excellent
Transverse mode	Defined by gain-guiding	Defined by gain-guiding	Defined by the optical cavity

Characteristics of X-ray RAFEL

- Large single-pass gain
- High reflectivity in a narrow energy band
- Saturate in a few passes
- Output pulses = a train of fs pulses separated by the cavity roundtrip time
- Output X-ray beams have both temporal and spatial coherence
- Optics re-image X-ray beam from the undulator exit to the undulator entrance
- High gain + small optical feedback = Saturation

X-ray RAFEL with Bragg Reflectors

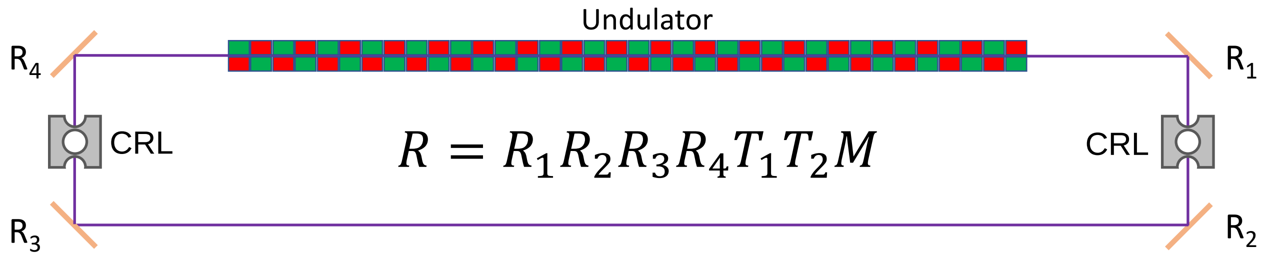

$R_1 R_2 R_3 R_4$ = Reflectivity of the Bragg reflectors within $\Delta\theta$

$T_1 T_2$ = Transmittivity of the two CRLs

M = Fraction of the return power that matches the FEL mode

RAFEL power in the n^{th} pass

$$P_n(z) = \frac{R P_{n-1}}{9} e^{\frac{z}{L_G}}$$

Bragg angle has to be slightly less than 45°

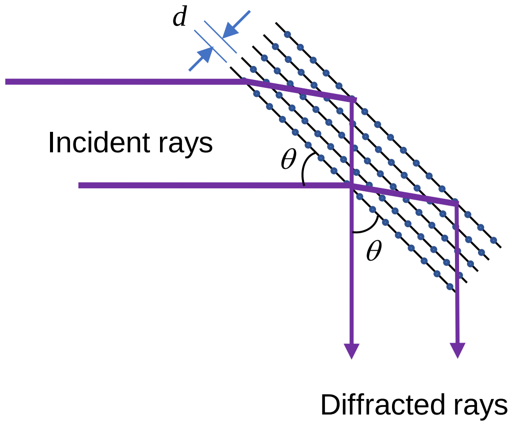

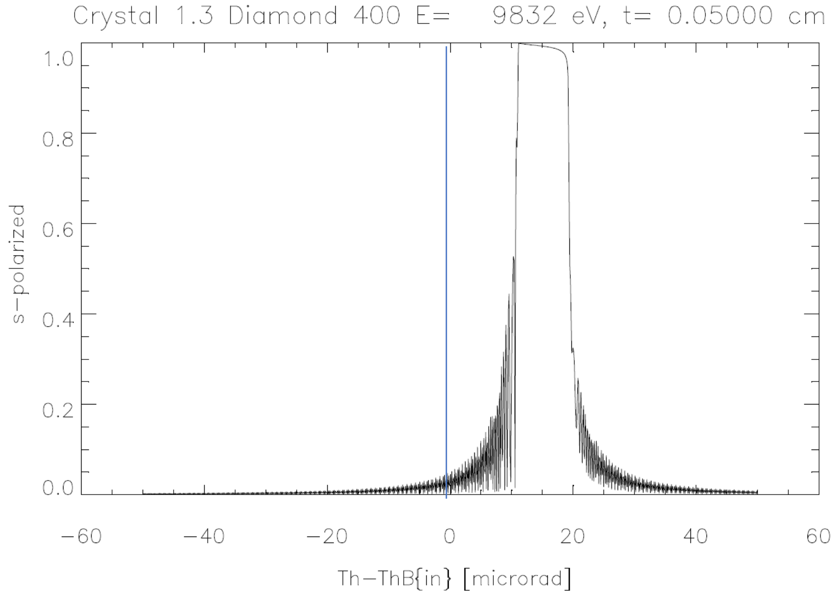

RAFEL Simulations with HXR Undulators

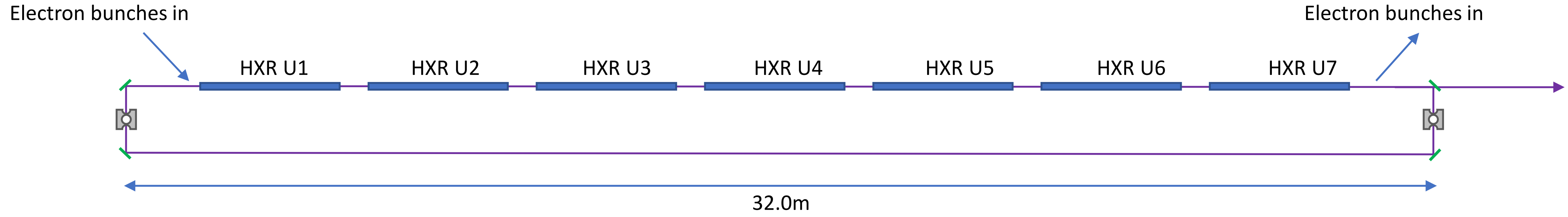

Electron beam energy-time

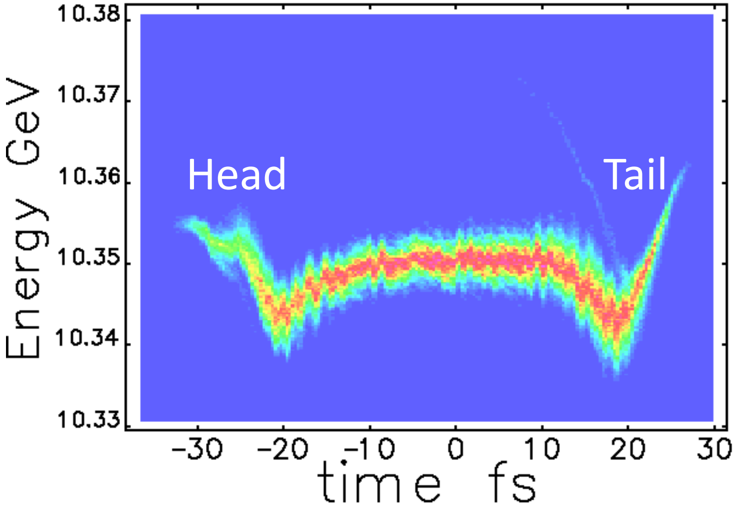

Current versus bunch coordinate

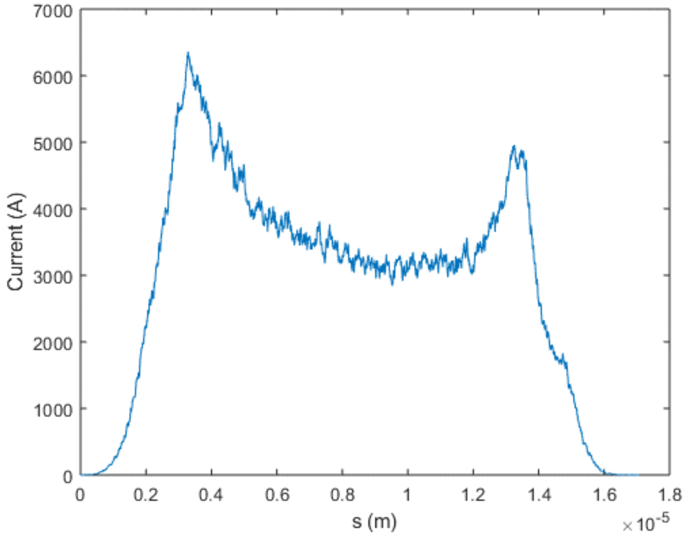

Radiation Electric Field after 1, 3 & 4 Diffractions

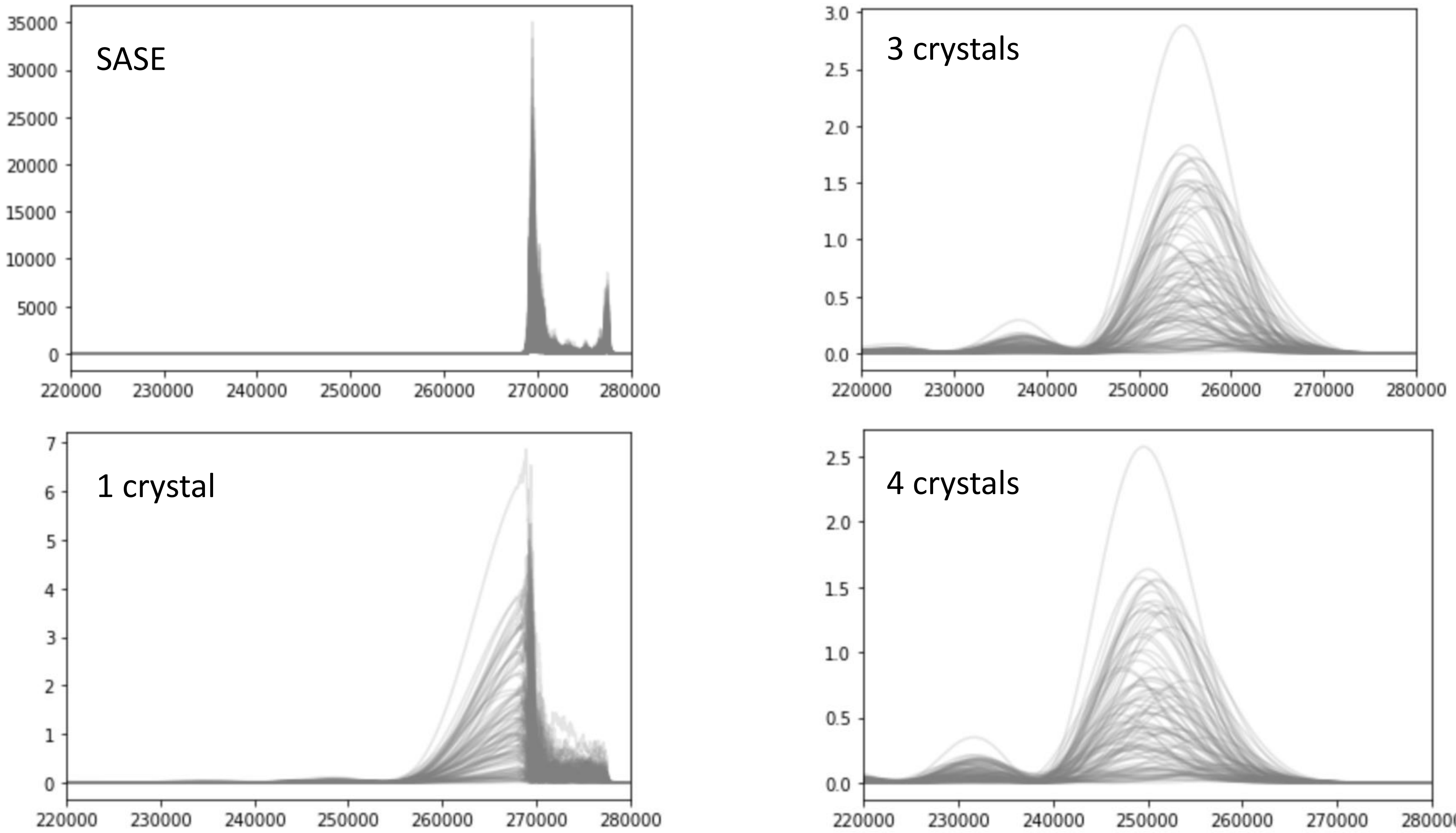

Expected Performance of X-ray RAFEL at LCLS

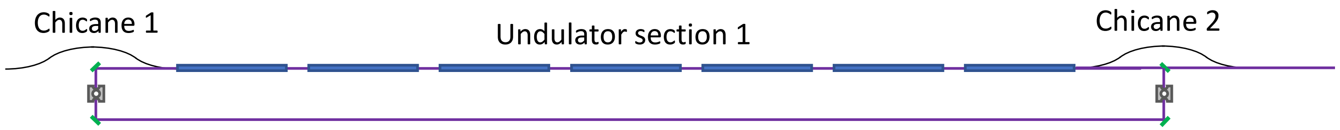

RAFEL power growth curve in 5 passes

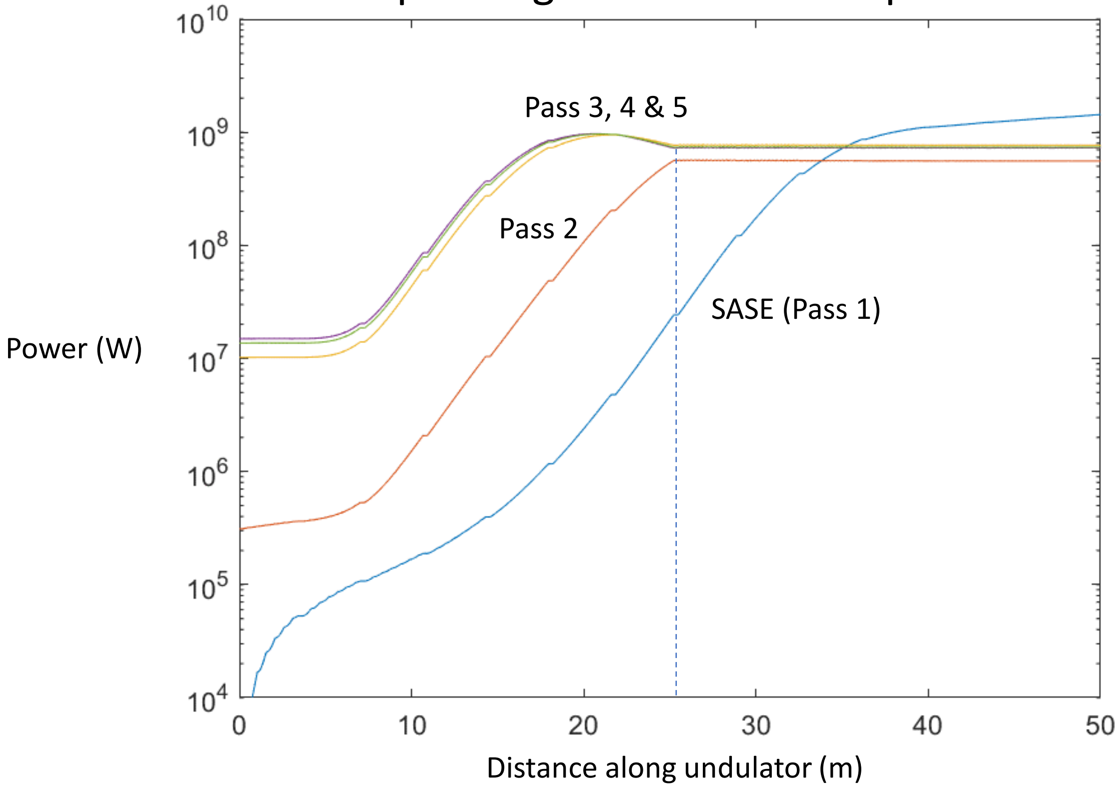

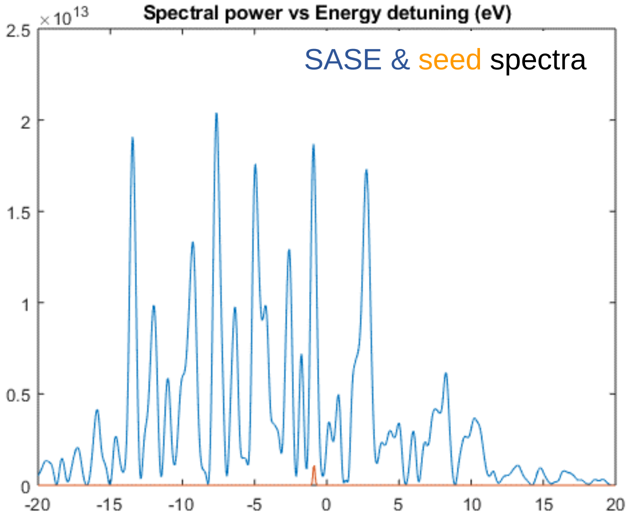

SASE in 1st Pass

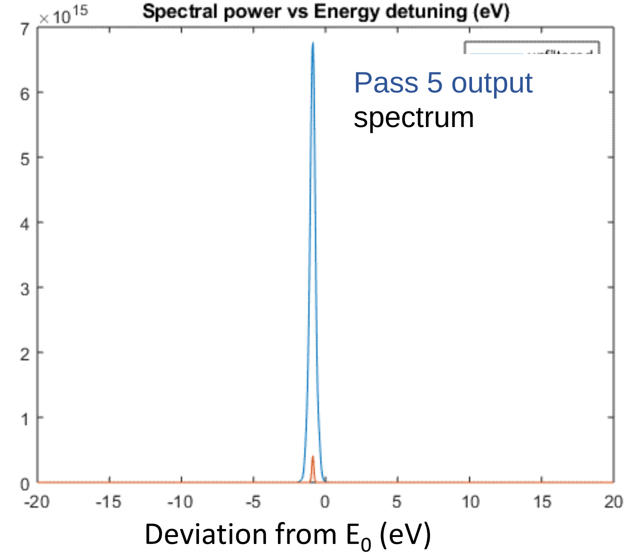

RAFEL in 5th Pass

Pass 1 (SASE) Filtering at 9.832 keV

Calculate the field spectrum (Fourier transform of radiation field versus time)

$$\mathfrak{I}(\omega) = \int_{-\infty}^{\infty} E(t)\, e^{-i\omega t} dt$$

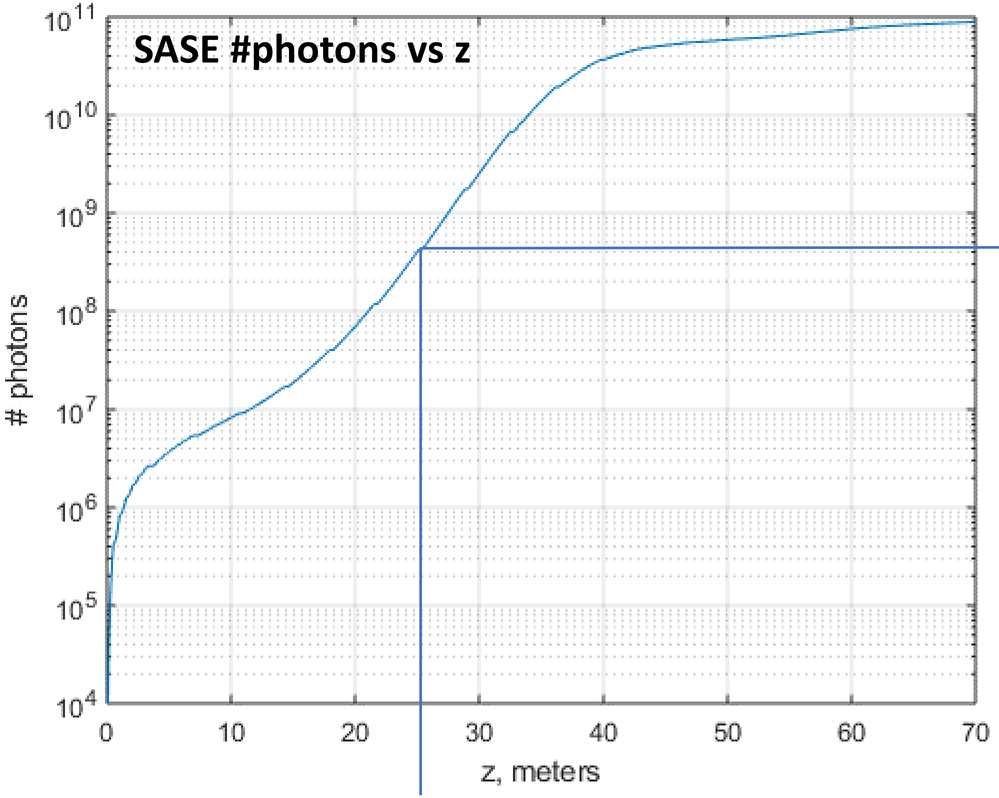

End of 7th HXU segment

$$\mathfrak{f}(\omega)\, \mathfrak{I}(\omega)$$

Field spectral filter

$$\mathfrak{f}(\omega) = F_0\, e^{-\frac{(\omega-\omega_0)^2}{2\sigma^2}}$$

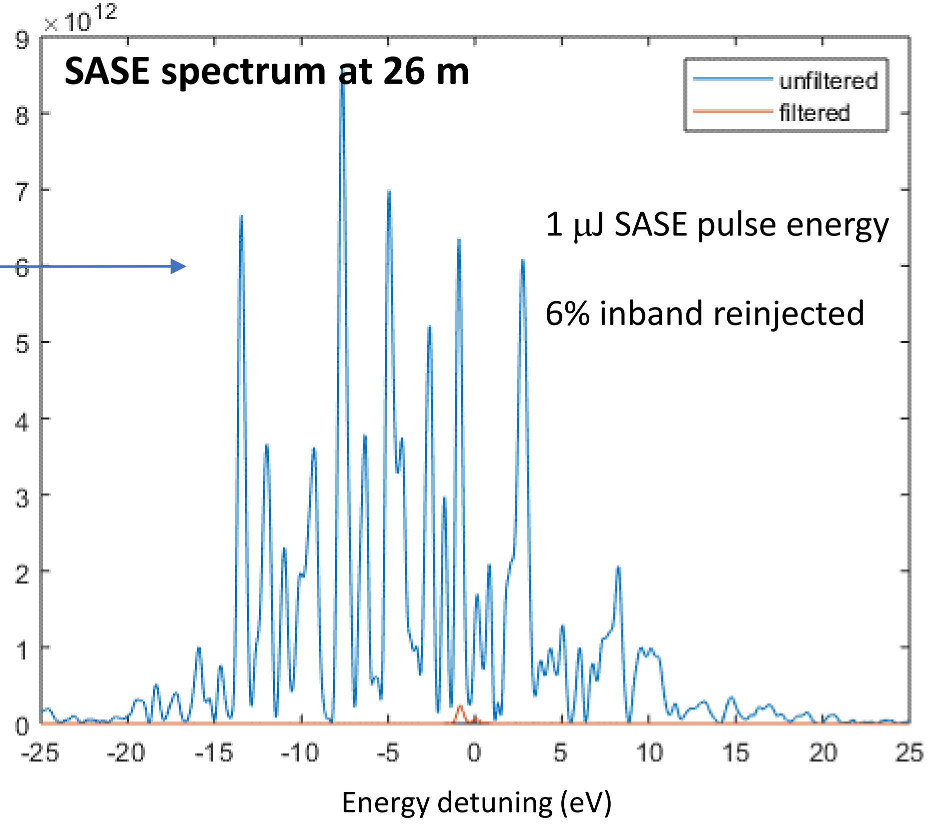

Pass 2 Number of Photons & BW at 9.832 keV

- 6% of the filtered SASE radiation at the end of the 7th HXU is reinjected
- Power grows to >10 GW in second pass
- Output spectrum has an rms bandwidth of 0.9 eV

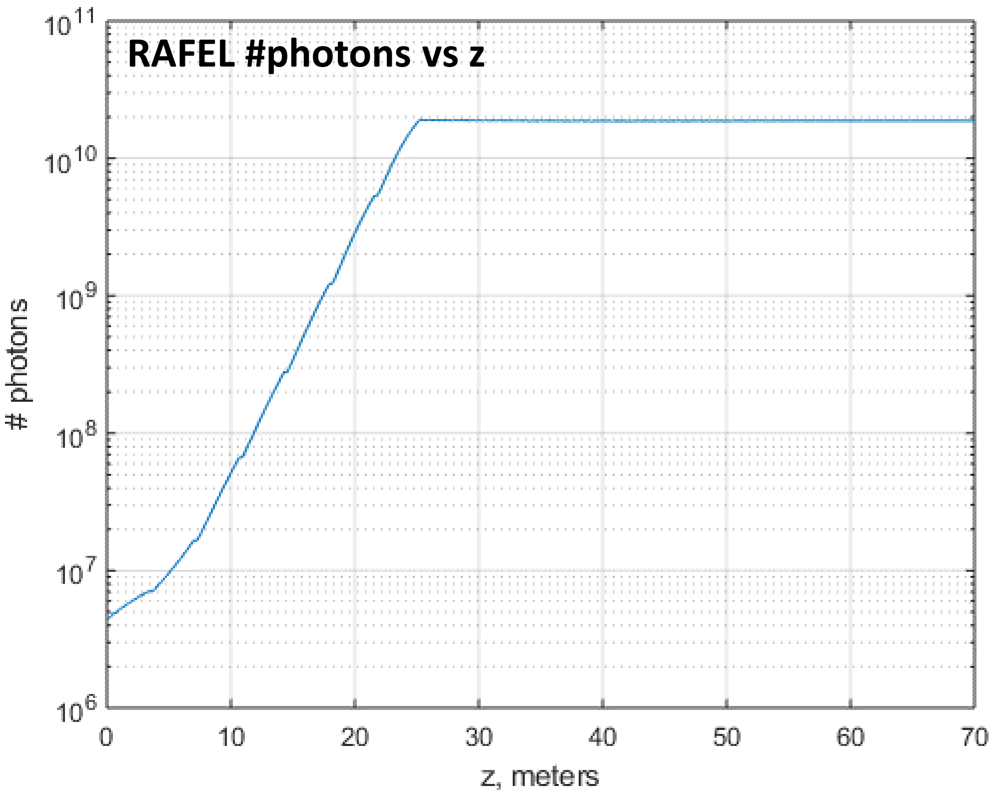

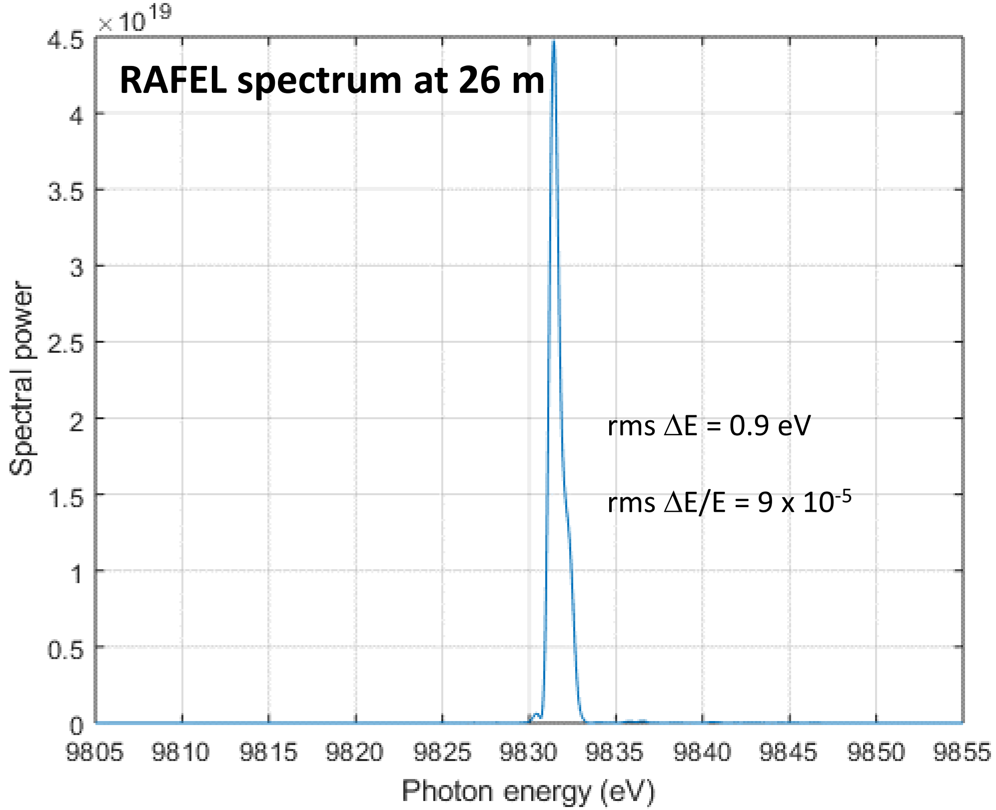

Pass 3 Number of Photons & BW at 9.832 keV

- 6% of the coherent radiation at the end of the 7th HXU in Pass 2 is reinjected
- Power saturates at the end of the 7th undulator
- Output spectrum has an rms bandwidth of 0.7 eV.

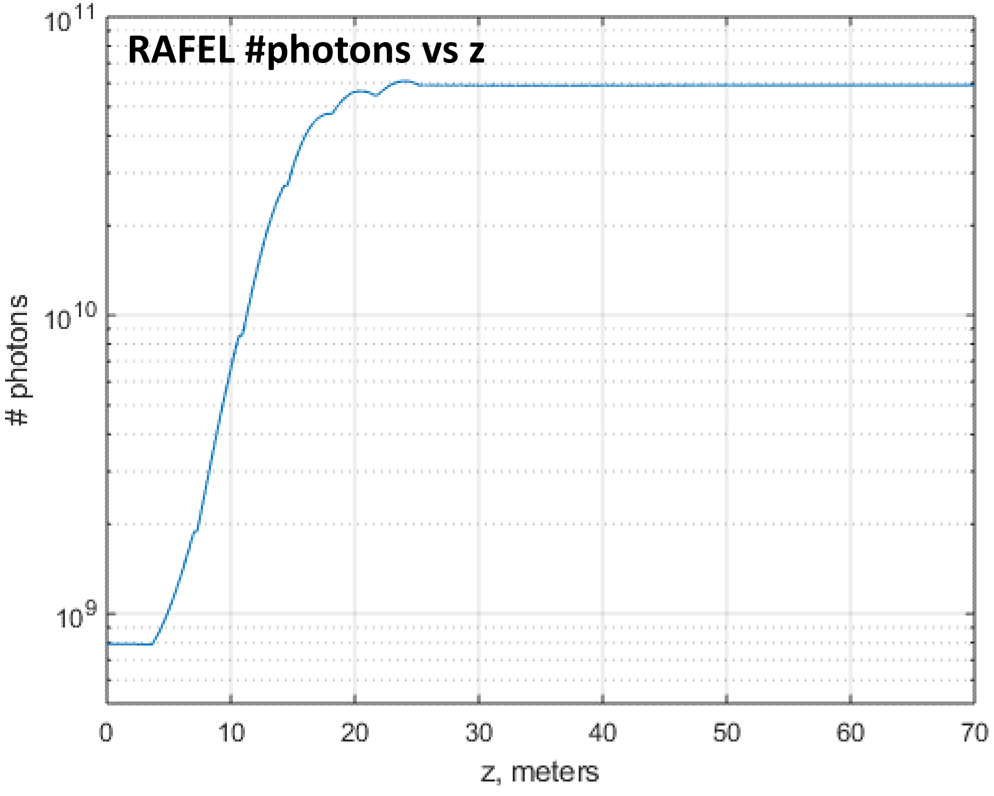

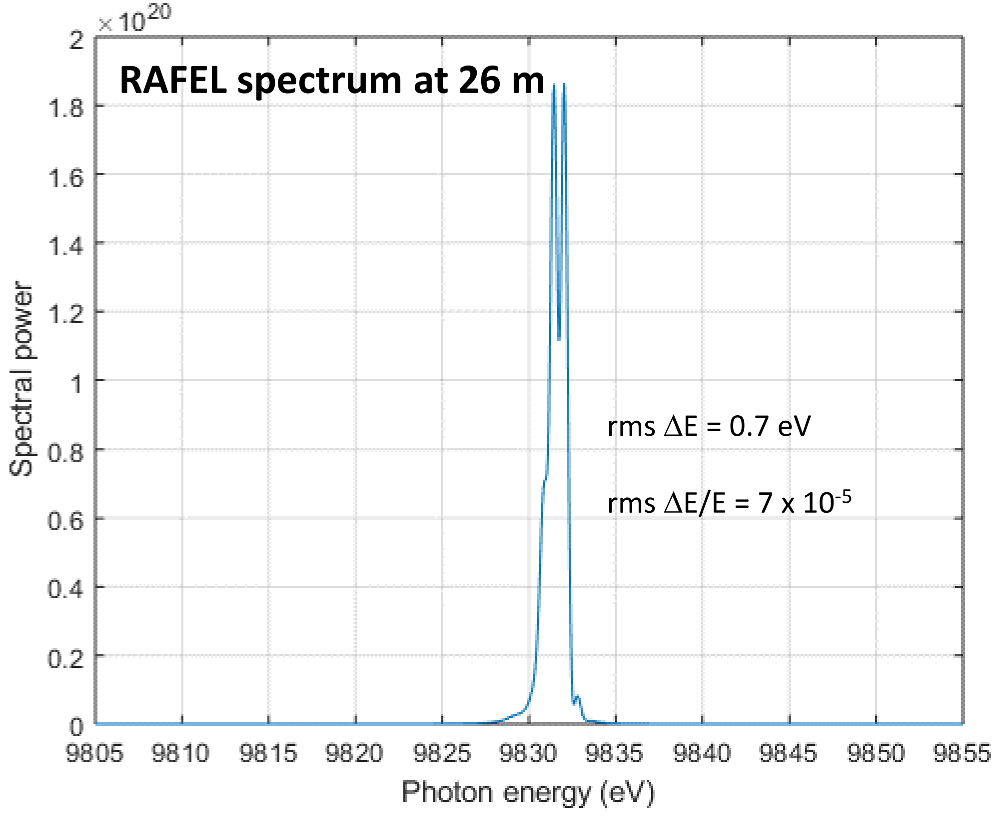

X-ray FEL Oscillator (XFELO)

SLAC NATIONAL ACCELERATOR LABORATORY

Los Alamos NATIONAL LABORATORY EST. 1943

X-ray FEL Oscillator (XFELO)

XFELO is the X-ray version of the FEL Oscillator
The first FEL (at 3.4 μm) was an FEL Oscillator

First Operation of a Free-Electron Laser*

D. A. G. Deacon,† L. R. Elias, J. M. J. Madey, G. J. Ramian, H. A. Schwettman, and T. I. Smith
High Energy Physics Laboratory, Stanford University, Stanford, California 94305
(Received 17 February 1977)

A free-electron laser oscillator has been operated above threshold at a wavelength of 3.4 μm.

Ever since the first maser experiment in 1954, physicists have sought to develop a broadly tunable source of coherent radiation. Several ingenious techniques have been developed, of which the best example is the dye laser. Most of these devices have relied upon an atomic or a molecular active medium, and the wavelength and tuning range has therefore been limited by the details of atomic structure.

Several authors have realized that the constraints associated with atomic structure would not apply to a laser based on stimulated radiation by free electrons.[1-5] Our research has focused on the interaction between radiation and an electron beam in a spatially periodic transverse magnetic field. Of the schemes which have been proposed, this approach appears the best suited to the generation of coherent radiation in the infrared, the visible, and the ultraviolet, and also has the potential for yielding very high average power. We have previously described the results of a measurement of the gain at 10.6 μm.[6] In this Letter we report the first operation of a free-electron laser oscillator.

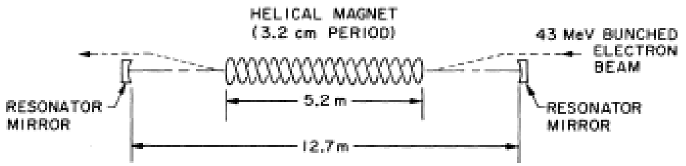

FIG. 1. Schematic diagram of the free-electron laser oscillator. (For more details see Ref. 6.)

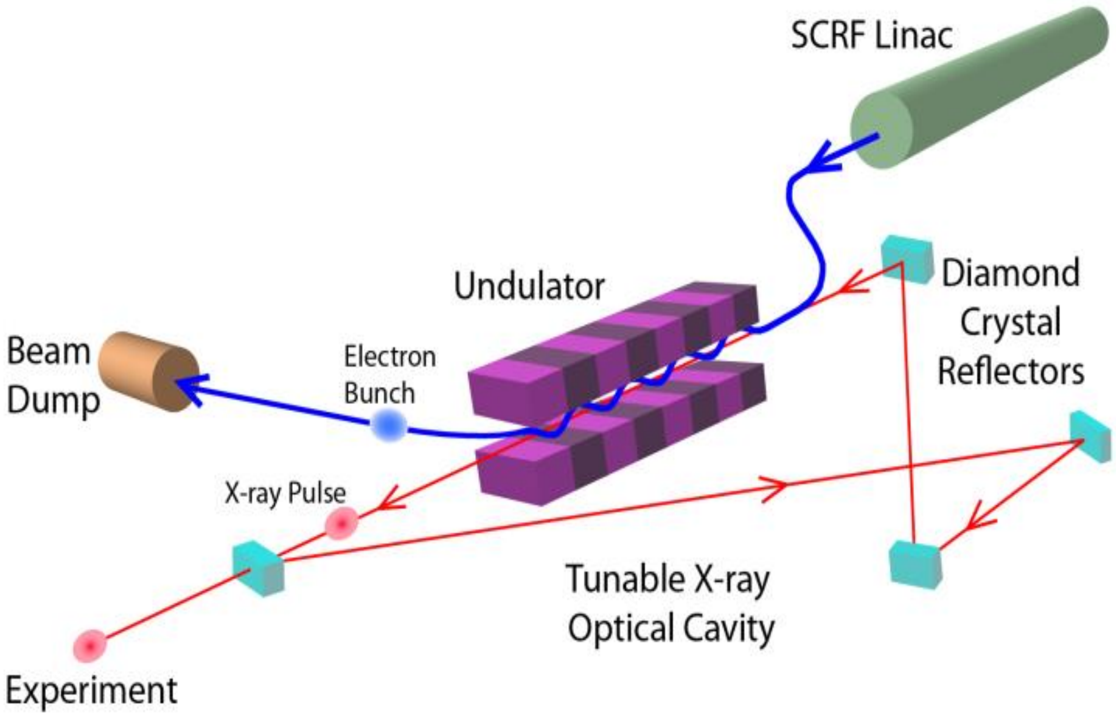

D.A.G. Deacon et al., Phys. Rev. Lett. 38, 892 (1977)

K.-J. Kim et al., Phys. Rev. Lett. 100 244802 (2008)
Yu. Shvyd'ko et al., Nature Photonics 5 (2011) 539

FEL Oscillator Glossary

- Small-signal gain (G_{SS})

$$P_{out} = (1 + G_{ss})P_{in}$$

- Saturated gain = Cavity loss

$$P_{out} = (1 + L)P_{in}$$

- Optical cavity

$$L_{cav} = \frac{c}{f_b}$$

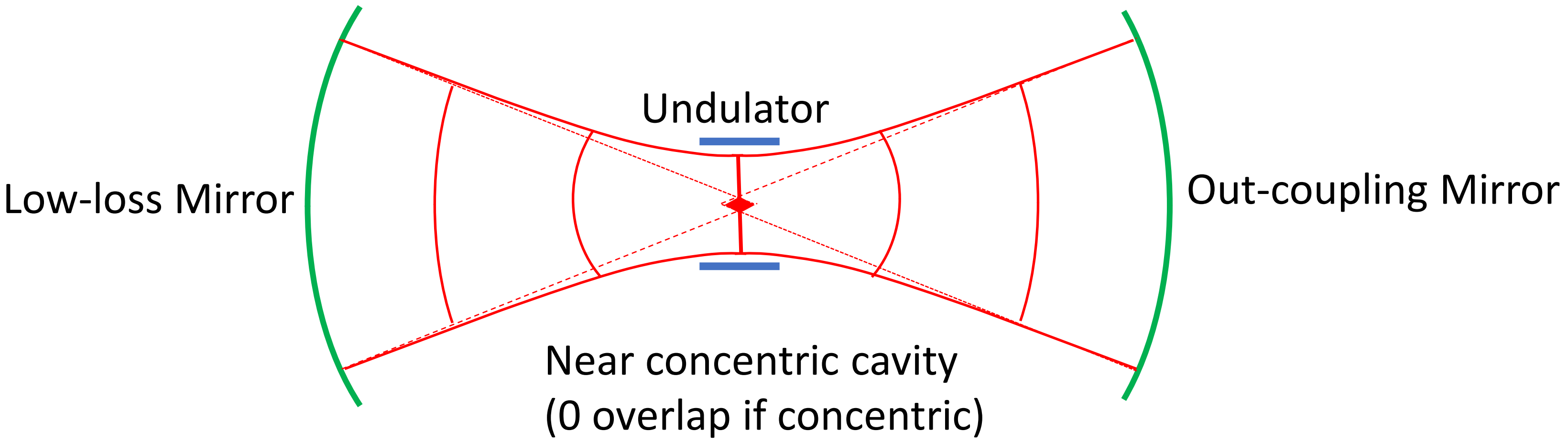

- Cavity loss = Out-coupling + Mirror absorption + Diffraction

FEL Oscillator Power Growth in Many Passes

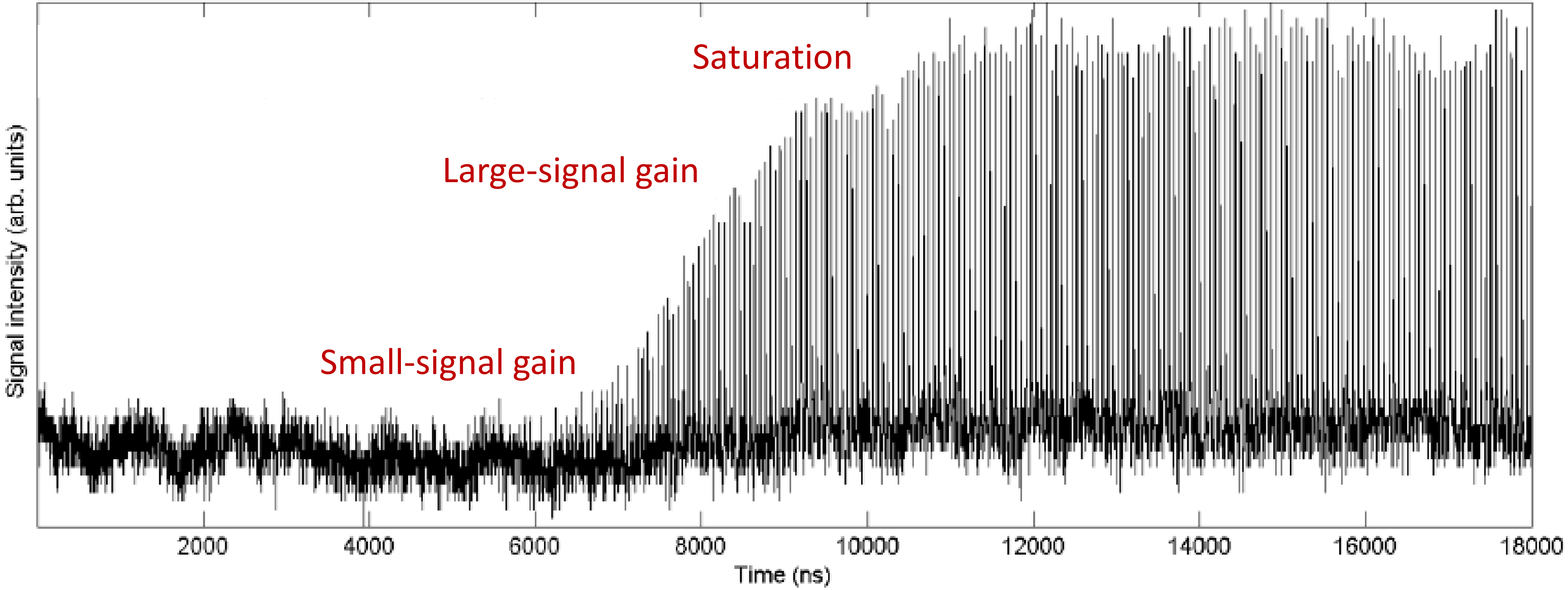

The small-signal gain is the highest single-pass gain
Gain decreases as the optical power grows (large-signal gain)
FEL saturates when intracavity power reaches the maximum

Maximum intracavity power

$$P_{in} = \frac{1}{2N_u} P_b$$

Courtesy of Andy Wolski, Introduction to FEL, CERN Accelerator School

Power & Gain versus Number of Passes

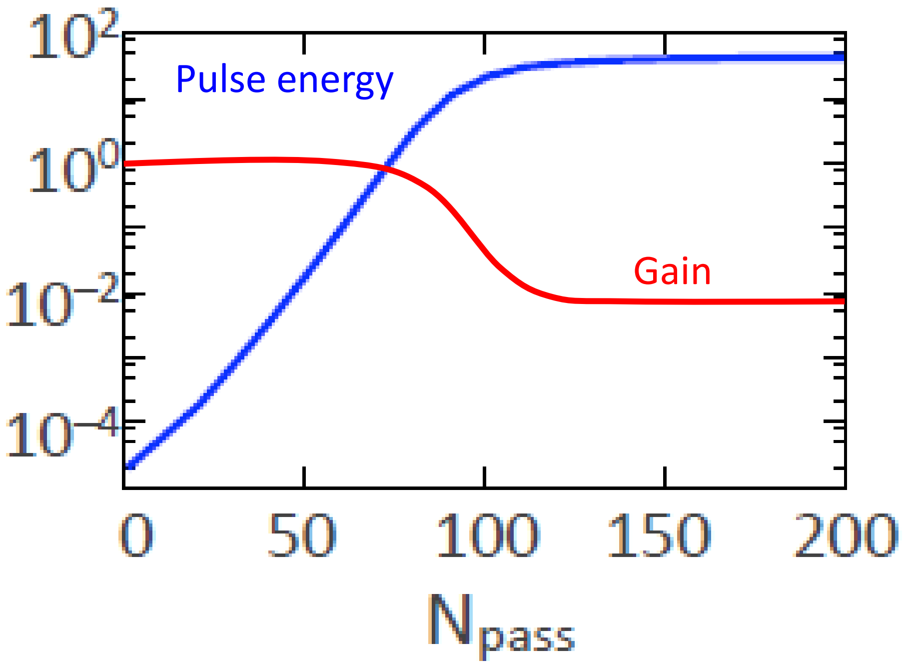

Start-up in an Oscillator is spontaneous emission

$$P_1 = P_s$$

Power as a function of pass number

$$P_n = R(1+G)P_{n-1} + P_s \qquad n \geq 2$$

$$P_n = \frac{\left(R(1+G)\right)^n - 1}{R(1+G) - 1} P_s$$

R is the net reflectivity of all cavity mirrors

Threshold condition $\quad R(1+G_{ss}) > 1$

Small-Signal Gain

The small-signal gain peaks at a longer wavelength than the resonant wavelength (at a fixed electron beam energy) or at higher energy than the resonant energy (at a fixed wavelength).

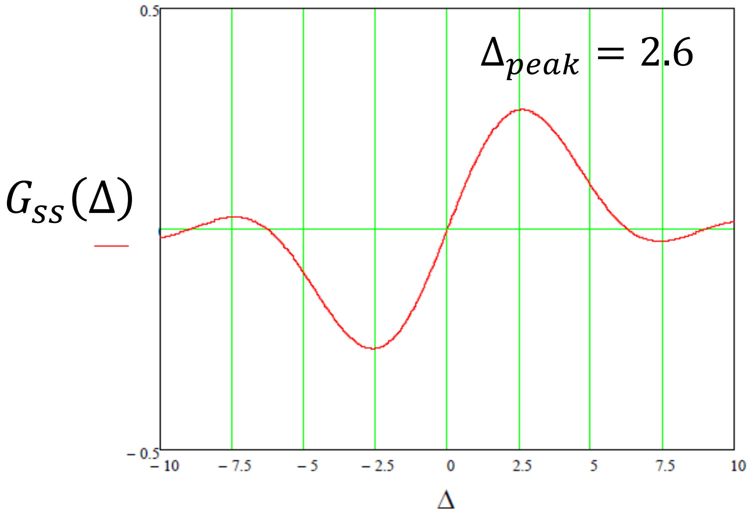

$$G_{ss}(\Delta) = \frac{4(4\pi\rho N_u)^3}{\Delta^3}\left(1 - \cos\Delta - \frac{\Delta}{2}\sin\Delta\right)$$

Detuning $\quad \Delta = \pi N_u \eta = 2\pi N_u \frac{\Delta\lambda}{\lambda}$

At the peak of the gain curve

$$\Delta = 2.6 \quad \Longrightarrow \quad G_{ss} = (0.0675)\, 4(4\pi\rho N_u)^3$$

Without length constraint, the small-signal gain scales with N_u^3

In reality, the undulator length is set at 1/3 the radiation Rayleigh range to avoid clipping the FEL beam as it diffracts and expands from the undulator center. It can be shown that $G_{ss} \sim N_u^2$

Large-Signal Gain & Saturation

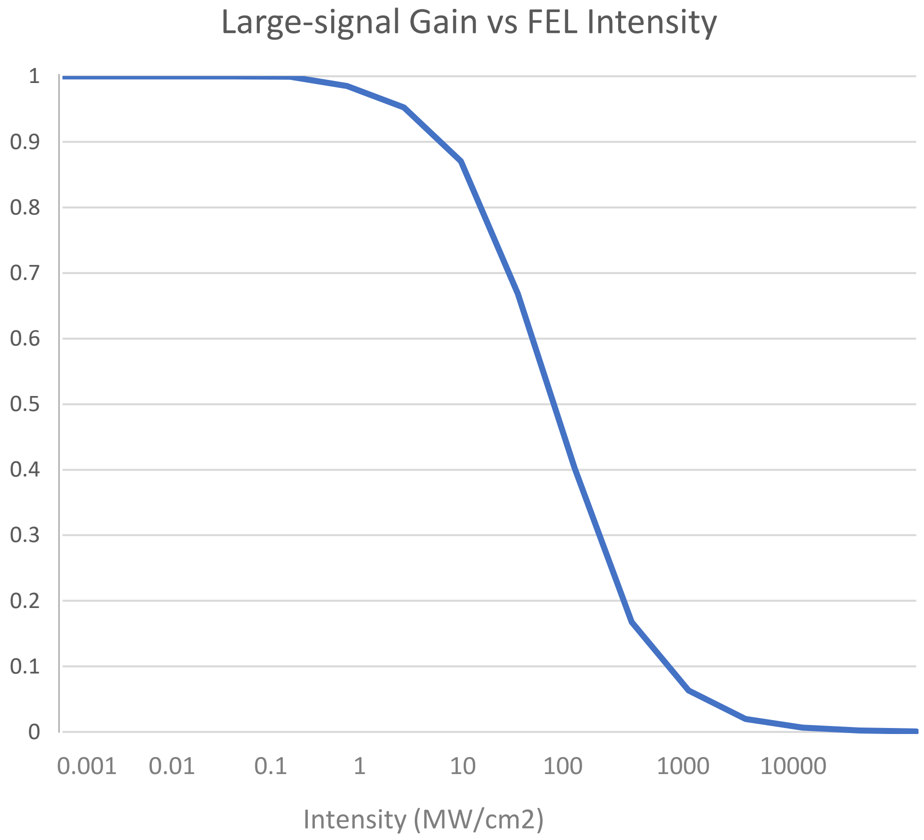

Gain decreases with intracavity FEL intensity

$$G(I) = \frac{G_{ss}}{1 + \left(\frac{I}{I_{sat}}\right)}$$

Saturated intracavity intensity

$$I_{sat}\left[\frac{MW}{cm^2}\right] \approx 100\pi \left(\frac{\gamma}{N_u}\right)^4 \frac{1}{\left(\lambda_u[cm]\widehat{K}\right)^2}$$

Output Coupling from XFELO Cavity

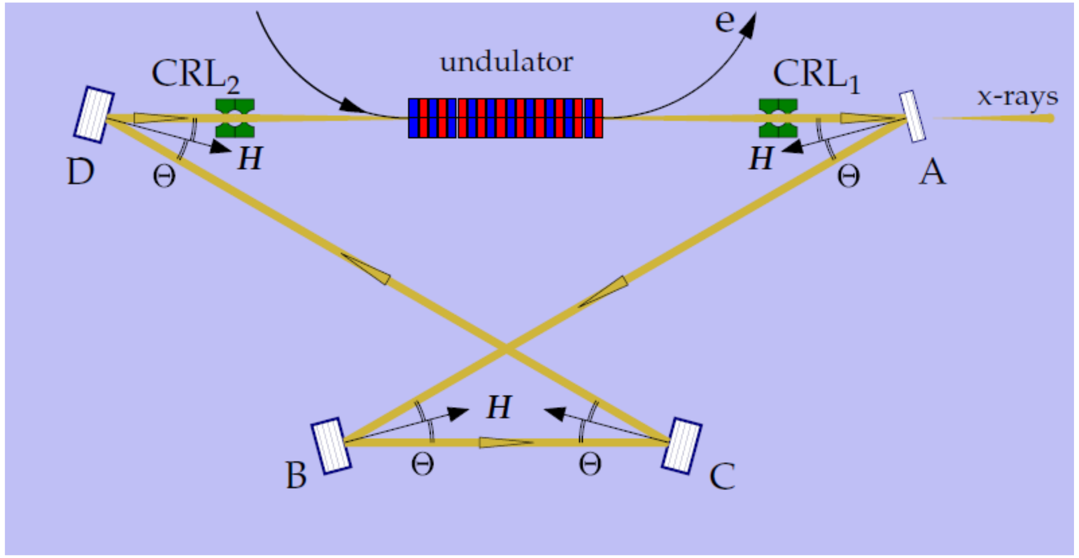

$$P_o = L_{out} P_{in}$$

Intracavity power $P_{in} = I_{sat} A_b$

Cavity loss

$$L = L_{out} + L_{abs} + L_{dif}$$

Out-coupling

Absorption

Diffraction

Drumhead crystal outcoupler

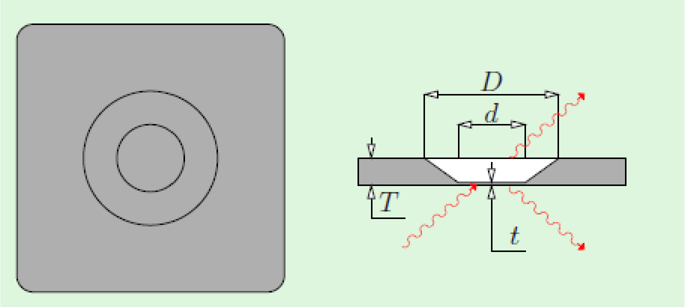

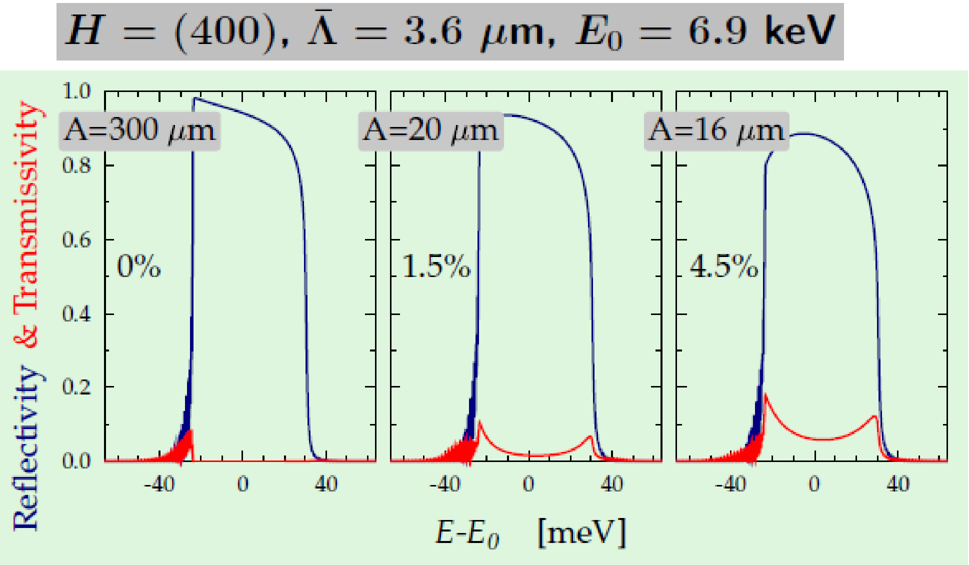

Y. Shvyd'ko, Phys. Rev. Accel. Beams, 22, 200703 (2019)

XFELO Pulse Shapes and Spectra vs. N_{pass}

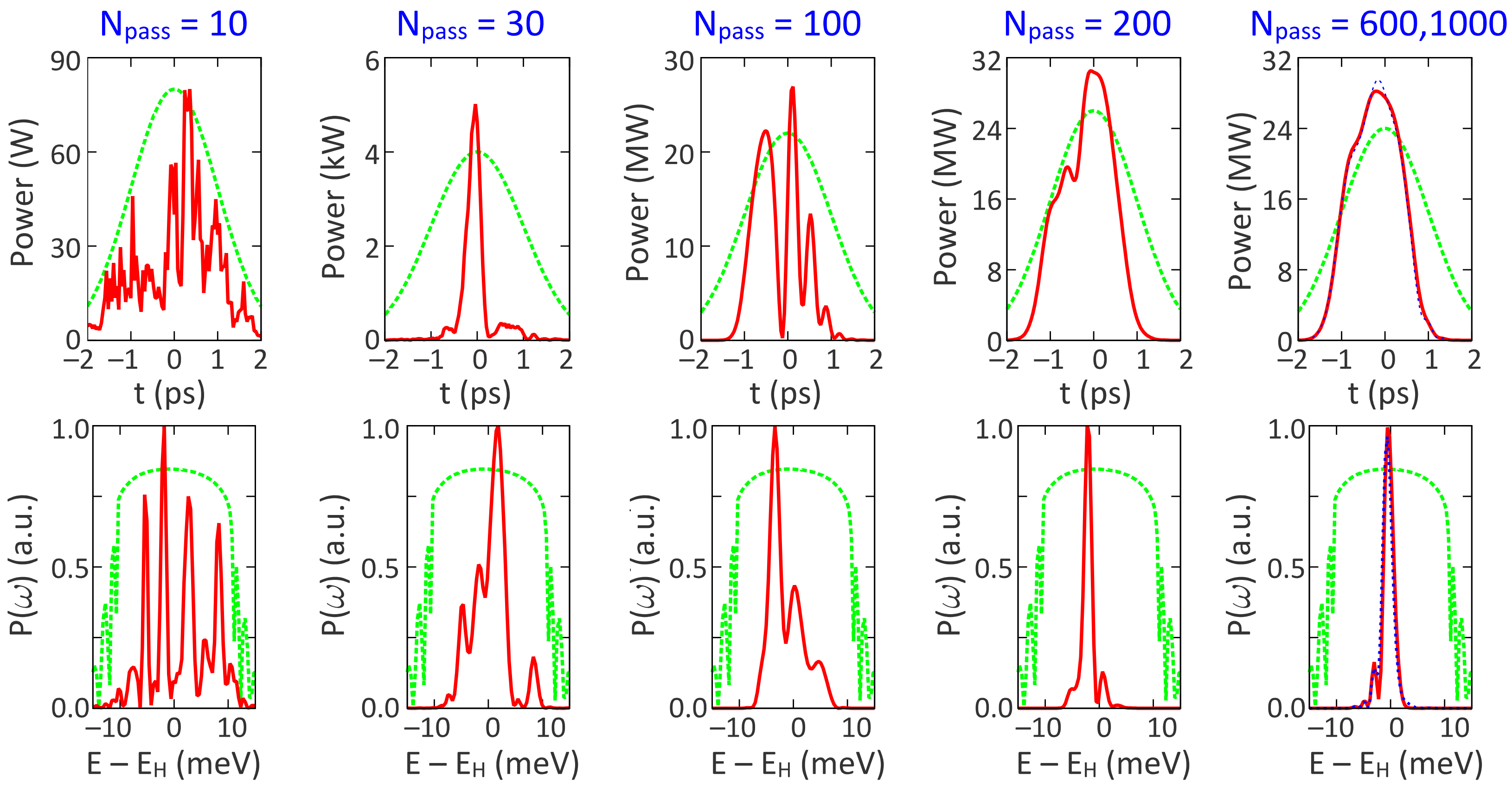

XFELO output spectra become narrower with N_{pass}

$$\left(\frac{\sigma_E}{E}\right) \sim \frac{1}{N_u} \frac{1}{\sqrt{N_{pass}}}$$

R.R. Lindberg et al., Phys. Rev. ST Accel. Beams, 14, 010701 (2011)

Summary

- Self-Seeding is an effective way to narrow the SASE FEL bandwidth. With fewer modes, Self-Seeding produces larger pulse-to-pulse energy fluctuations than SASE.
- Hard X-ray Self-Seeding uses the Forward Bragg Diffraction to create a notch in the SASE spectrum, resulting in coherent wake pulses in the time domain. One of these wake pulses is amplified by “fresh bunches” of electrons in subsequent undulators.
- Soft X-ray Self-Seeding uses a grating and a slit to select a narrow band of the SASE output to seed the next undulator section.
- Regenerative Amplifier FEL has been demonstrated in the IR. An on-going effort at SLAC is aimed at demonstrating RAFEL and XFELO in the hard X-ray region.
- XFELO extends the FEL Oscillator wavelengths from IR, visible and UV to the X-ray region. XFELO can potentially achieve Transform-limited bandwidth of a few meV.